

Emergent Dynamics of Neuronal Networks with Differing Time-scales and Modular Structure

A Thesis

submitted to

Indian Institute of Science Education and Research Pune
in partial fulfillment of the requirements for the
BS-MS Dual Degree Programme

by

Kunal Mozumdar

Reg. No. : 20121023



Indian Institute of Science Education and Research Pune
Dr. Homi Bhabha Road,
Pashan, Pune 411008, INDIA.

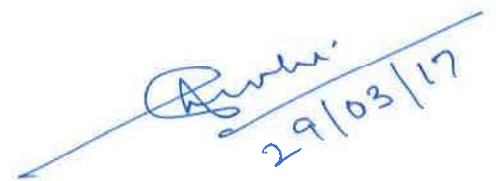
May, 2017

Supervisor: Prof. G. Ambika
© Kunal Mozumdar 2017

All rights reserved

CERTIFICATE

This is to certify that this dissertation entitled *Emergent Dynamics of Neuronal Networks with Differing Time-scales and Modular Structure* submitted towards the partial fulfillment of the BS-MS dual degree programme at the Indian Institute of Science Education and Research, Pune represents study/work carried out by **Kunal Mozumdar** at Indian Institute of Science Education and Research under the supervision of **Prof. G. Ambika**, Professor Department of Physics during the academic year 2016-2017.

A handwritten signature in blue ink, appearing to read 'Ambika', is written over a horizontal line. Below the signature, the date '29/03/17' is written in blue ink.

Prof. G. Ambika

Committee:

Prof G. Ambika

Dr. Collins Assisi

This thesis is dedicated to my grandparents.

DECLARATION

I hereby declare that the matter embodied in the report entitled *Emergent Dynamics of Neuronal Networks with Differing Time-scales and Modular Structure* are the results of the work carried out by me at the Department of Physics, Indian Institute of Science Education and Research, Pune, under the supervision of **Prof. G. Ambika** and the same has not been submitted elsewhere for any other degree.

Date: 29th March 2017



Kunal Mozumdar

Acknowledgments

I would like to thank Prof. G. Ambika for her guidance and supervision and my lab members - Snehal Shekatkar, Dinesh Choudhary and Sandip V.G. for useful insights in my thesis work. I would also like to acknowledge my brother for assisting with the diagrams in this text, my parents for their blessings and friends especially Prashali Chauhan, Varun Shrivastava, Gaurav Khairnar and every person in the physics student room for the intellectual discussions and for making this an enjoyable exercise. And finally coffee for making me reach this far. I would also thank the DST-Inspire program, IISER and Physics Department for providing the necessary resources to accomplish this.

Abstract

The dynamics of the mammalian brain is captured using nonlinear dynamics in the framework of complex networks. We study the dynamics of Hindmarsh-Rose neurons with time-scale mismatch in detail, for both simplistic and realistic network models and develop various schemes for characterizing the collective dynamics of the neurons. For a simple system with two mutually coupled neurons with differing time-scales, we observe that the difference in timescales leads to synchronized states of frequency suppression. In a ring of HR neurons, with time-scales decreasing sequentially, we find the neurons go into Synchronized Frequency Suppressed Clusters.

We extend our model to more realistic models of neuronal networks like modular networks. Modular networks of HR neurons show various interesting dynamical states like de-synchronized states, phase synchronization and activity death states. Further characterization of frequency suppressed states in such networks can lead to better understanding of coding of information in neuronal networks.

Contents

Abstract	xi
1 Introduction	5
1.1 Hodgkin-Huxley model of Neurons	6
1.2 FitzHugh-Nagumo Neuron Model	8
1.3 Hindmarsh-Rose Neuron model	9
1.4 Coupling in Neurons	12
1.5 Outline of Study	16
2 Mutually Coupled Slow and Fast Neurons	17
2.1 Coupled Neurons with differing Time-scales	17
2.2 Calculation of Burst Frequency	19
2.3 Dynamics of Coupled Slow and Fast Neurons	20
3 Dynamics of HR Neurons on Regular Networks	25
3.1 Ring of HR neurons	25
3.2 Dynamics of Neurons on a Ring	27
3.3 Summary	28

4	Modular Networks of HR Neurons	31
4.1	Generating Modular Networks	32
4.2	Modular Neuronal Networks	33
4.3	Dynamical States in Modular Neuronal Networks	35
4.4	Case 1 : Assortative Excitatory Networks	37
4.5	Case 2 : Disassortative inhibitory Networks	40
5	Conclusions	45
5.1	Future Prospects	47

List of Figures

1.1	Schematic diagram of a typical neuron	6
1.2	Phase portrait of FitzHugh-Nagumo neuron showing the different dynamical states.	9
1.3	$I_e = 1.5$, Spiking dynamics	10
1.4	$I_e = 2.5$, Regular square bursts	11
1.5	$I_e = 3.0$, Chaotic bursts	11
1.6	$I_e = 1.5, b = 2.5$, Plateau like bursts - 1	11
1.7	$I_e = 4, b = 2$ Plateau like bursts - 2	12
1.8	Parameter plane $I_e - b$ showing the various bursting states of the HR neurons. The colour code on the right represents the average number of spikes in between each bursts. Dark blue region corresponds to fixed points or spiking, Blue region corresponds to square bursting, light blue, yellow and orange region to plateau like bursting and red region corresponds to a region of continuous high frequency bursts.	12
1.9	Schematic diagram of a synaptic transmission	13
1.10	Synaptic coupling function Γ plotted for different values of x_1 and x_2	14
1.11	Synchronization in two mutually coupled chaotically bursting HR neurons. We see that at same value of g_s the electrically coupled neurons are completely synchronized whereas the synaptically coupled neurons are in phase synchronization.	15
1.12	Amplitude death at $g_s > 2$ for synaptically coupled chaotic bursting HR neurons.	15

2.1	Mutually coupled neurons	18
2.2	Time-series of x_i . Increasing the coupling strength from (a-d) for a constant η we find the systems tending towards a frequency synchronized state. But there is no state of complete synchronization for them.	20
2.3	Regions of frequency synchronization for spiking neuron at $I_e = 1.5$. Red region corresponds to FD , Green region corresponds to FS and Blue region corresponds to AD	21
2.4	Regions of frequency synchronization for chaotic bursting neuron at $I_e = 3$. Red region corresponds to FD , Green region corresponds to FS and Blue region corresponds to AD . We observe a broader region of FD as the intrinsic dynamics is chaotic to begin with.	21
2.5	Regions of frequency synchronization for chaotic bursting neurons at $I_e = 3$ coupled electrically. We observe an absence of AD in this case. This shows that nonlinear coupling causes AD in neurons, not timescale mismatch.	22
2.6	Frequency suppression in regularly spiking neurons, $I_e = 1.5$	23
2.7	Frequency suppression in chaotic bursting neurons, $I_e = 3$	23
3.1	Ring of neurons with differing time-scales	26
3.2	Frequency of each isolated neuron when $g_s = 0$ and $\Delta\eta = 0.02$	28
3.3	Frequency suppressed clusters for a ring of neurons with increasing coupling strength. In both these cases, there are clusters of frequency synchronized neurons which finally collapse into a single cluster of SFSS as the coupling strength increases.	29
3.4	Frequency suppressed state for a ring of 100 neurons with $\Delta\eta = 0.005$. There are no distinct clusters present, the system has a continuous transition in frequency	30
4.1	Adjacency matrix of a Associative Excitatory Network. Neurons in a module have higher number of synapses from within the module, than from outside. Hence the network has denser excitatory connections than inhibitory ones.	34
4.2	Adjacency matrix of Disassociative Inhibitory Network. All to all inhibitory connections between the modules with sparse excitatory connections.	35

4.3	Desynchronized neurons in AEN: At very high values β the system is usually desynchronized. This is because inhibitory coupling breaks the phase synchrony between the modules	39
4.4	Synchronized States in AEN: At certain values of α and β we get states like these where two modules are synchronized in phase and the others are in off phase. (a) Module 1 and 2 are PS and 2 and 4 are in PS. (b) Module 1 and 3 are PS	39
4.5	Change in β can revive the network from AD to Desynchronized State. We increase the value of β for a constant α to force the system to burst. So essentially the inhibitory coupling can revive a system from activity death state.	40
4.6	$\alpha - \beta$ parameter plane for Ω_1 . Red shades correspond to Desynchronised States, Blue shades corresponds to Phase Synchronized States, Green shades corresponds to Activity death states. The numbers given in the vertical band represent the dynamical states: 1- DS-4 , 2- DS-3 , 3- DS-2 , 4- DS-2,P-2 , 5- DS-1 , 6- TB , 7- PS-2 , 8- PS-2,2 , 9- PS-3 , 10- PS-4 , 11- AD-1 , 12- AD-2 , 13- AD-3 , 14- AD-4 , 15- AD	41
4.7	Mixed-mode oscillations observed in DIN. The figure has been plotted for $\alpha = 0.3$ and $\beta = 0.1$ and consists of the time series of 4 neurons belonging to different modules. We find that each individual neuron exhibits small and large amplitude bursts.	42
4.8	Travelling bursts in the modular network. (a) For $\alpha = 0$ the spikes inside each burst are completely synchronized. (b)For $\alpha > 0$ the spikes inside the burst become irregular. Bursting of neurons in each module is phase synchronized, but each module bursts successively after the other appearing dynamically as travelling bursts.	42
4.9	(a) Desynchronized State, (b) Activity Death State. High value of α desynchronizes the network.	43
4.10	$\alpha - \beta$ parameter plane for Ω_2 . Red shades correspond to Desynchronised States, Blue shades corresponds to Phase Synchronized States, Green shades corresponds to Activity death states. The numbers given in the vertical band represent the dynamical states: 1- DS-4 , 2- DS-3 , 3- DS-2 , 4- DS-2,P-2 , 5- DS-1 , 6- TB , 7- PS-2 , 8- PS-2,2 , 9- PS-3 , 10- PS-4 , 11- AD-1 , 12- AD-2 , 13- AD-3 , 14- AD-4 , 15- AD	43

Chapter 1

Introduction

The *Brain* is the most complex and efficient computational device created and perfected by nature. This system just like any other computer is capable of detecting and processing various stimuli from the external and internal environment and producing a unique response for the different stimuli received. It also stores information as memory and retrieves it for later uses. Along with these, it is also capable of generating complex emergent behavioural aspects of cognition, emotions, self-awareness and imagination. This versatility of Brain intrigued biologists, physicist, mathematicians, computer scientists and engineers alike to find a mechanism for how it does what it does and can we recreate it artificially.

The nervous system achieves the remarkable ability to do computations due to intricate networks of cells called *neurons*. Ramon y Cajal first observed neurons in 1888. Neurons are excitable systems which tend to show a change in their intrinsic dynamics based on the inputs from the external environment. They generate what is called as an *action potential* or spikes in response to the external stimulus. At a cellular level, this behaviour is the result of the activity of various voltage-gated ion channels present on the surface of the membrane of the neuron which causes depolarization and re-polarization of the membrane potential occurring in the time scale order of milliseconds. This looks like a delta function or a spike in the membrane potential of the neuron which is termed as an action potential. [1]

A schematic diagram of a typical neuron with its associated parts is shown in fig 1.1. In a typical case, the action potential starts from the tip of the axon and propagates throughout the axon and finally terminates in the synapse releasing neurotransmitters. These neuro-

transmitters reach the respective receptors at the dendrites of other neurons triggering action potentials in them. Single neurons can exhibit a variety of behaviour depending on the external input, their morphological structure and diversity and distribution of ion channels present on their surface.

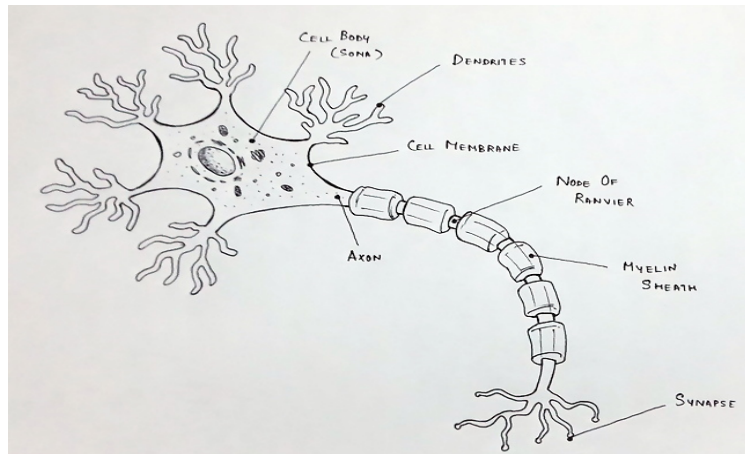


Figure 1.1: Schematic diagram of a typical neuron

1.1 Hodgkin-Huxley model of Neurons

The study of neuroscience was restricted to scientists studying medicine or physiology, until the early 1900s when neurons were represented as electrical circuits, and mathematical models for neuronal activity were developed. There were several mathematical models for neurons in several contexts depending on the type of system being modelled. But the most accurate and detailed prescription of neurons till date is the Hodgkin and Huxley model of neurons.

Alan L. Hodgkin and Alfred F. Huxley gave their mathematical model for the neuronal activity in 1952. This model describes the activity of the Giant Squid Axon using a set of nonlinear differential equations. It essentially is a conductance-based model which accounts for all the voltage-gated ion channels and passive channels present on the neuronal membrane. Hodgkin-Huxley model assumed the neuron to be equivalent to an RC circuit where the membrane of the neuron acts as capacitor as it stores charges across its surface and the ion channels represent variable conductors. They also developed a novel mechanism for the functioning of the ion channel by introducing the gating variables. These gating variables

represent the probability of the gates to be open or closed at a given time. The HH model for the giant squid axon is given by the following equations. [2]

$$C_m \dot{V} = \bar{g}_K n^4 (V_K - V) + \bar{g}_{Na} m^3 h (V_{Na} - V) + \bar{g}_l (V_l - V) + I_e \quad (1.1.1)$$

$$\dot{n} = \alpha_n (1 - n) - \beta_n n \quad (1.1.2)$$

$$\dot{m} = \alpha_m (1 - m) - \beta_m m \quad (1.1.3)$$

$$\dot{h} = \alpha_h (1 - h) - \beta_h h \quad (1.1.4)$$

Now in these equations variables V, n, m and h represent the *membrane potential* of the neuron and the *gating variables* for Pottassium and Sodium resepectively. Parameter C_m is capacitance across the membrane. Other parameters like \bar{g}_X represent the conductance of the channel, I_e is the external input current and V_X is the threshold potential or reversal potential of the ion channel. α and β are the rates of opening and closing of the gates and are functions of membrane potential and time given as:

$$\alpha_n = 0.01 \left(\frac{10 - V}{\exp\left(\frac{10 - V}{10}\right) - 1} \right) \quad \beta_n = 0.125 \exp\left(\frac{-V}{80}\right) \quad (1.1.5)$$

$$\alpha_m = 0.1 \left(\frac{25 - V}{\exp\left(\frac{25 - V}{10}\right) - 1} \right) \quad \beta_m = 4 \exp\left(\frac{-V}{18}\right) \quad (1.1.6)$$

$$\alpha_h = 0.07 \exp\left(\frac{-V}{20}\right) \quad \beta_h = \left(\frac{1}{\exp\left(\frac{30 - V}{10}\right) + 1} \right) \quad (1.1.7)$$

This model is a very detailed way of describing the dynamics of the neurons. It accounts for the functioning of each ion channel and incorporating it into the dynamical behaviour of the neurons. In cases where there are other ion channels and currents present like the voltage gated Calcium channels or the hyperpolarising currents we can add more gating variables and if the gate structure and properties are known we can write the differetial equations for them [3]. Also this model is experimentally verifiable as the parameters V_X, C_m and the rates α, β can always be tallied with experiments.

Hodgkin-Huxley model essenatially made neuroscience a subject for physicists and mathematicians to ponder upon, as these cells are now seen as oscillators and their dynamics could be reduced to differential equations. HH model has been used in several systems and varia-

tions of this has been widely used to study dynamics of neurons and neuronal networks.

1.2 FitzHugh-Nagumo Neuron Model

HH model is a complicated model for a single neuron with 4 or more coupled nonlinear differential equations, more than 6 functions and more than 7 parameters. This was the motivation for finding simpler models of neurons which showed the spiking behaviour.

One of the models is the FitzHugh-Nagumo model presented by Richard FitzHugh in 1961 [4], and the equivalent circuit for the model was given by Nagumo in 1962 [5]. FitzHugh Nagumo model is given as:

$$\dot{v} = v - \frac{v^3}{3} - w + I_e \tag{1.2.1}$$

$$\dot{w} = \epsilon(v + \alpha - \gamma w) \tag{1.2.2}$$

The variable v corresponds to the membrane potential i.e. the fast variable and variable w is the slow gating variable (sodium channel in neurons). The parameter I_e is external current given to the neuron and other parameters are α , ϵ and γ where $0 < \alpha < 1$ and $\epsilon \ll 1$ (accounting for the slow kinetics of the sodium channel).

FitzHugh-Nagumo model (FHN) is one of the simpler models of excitable oscillators like neurons but it is not able to provide a realistic description of the action potentials. Also the FitzHugh Nagumo model was not able to give a relationship between the frequency and applied current. Hence there were several attempts to give better models for neurons. This led to a 2-dimensional model proposed by J.L. Hindmarsh and R.M. Rose in 1982 [6] , which modifies the FHN model to produce spiking behaviour. Hindmarsh and Rose further modified their own model by introducing a third variable which evolves slowly, to produce bursting behaviour in the neurons [7]. Following section presents a detailed account of the dynamics of 3 variable HR neurons using analytical and numerical techniques.

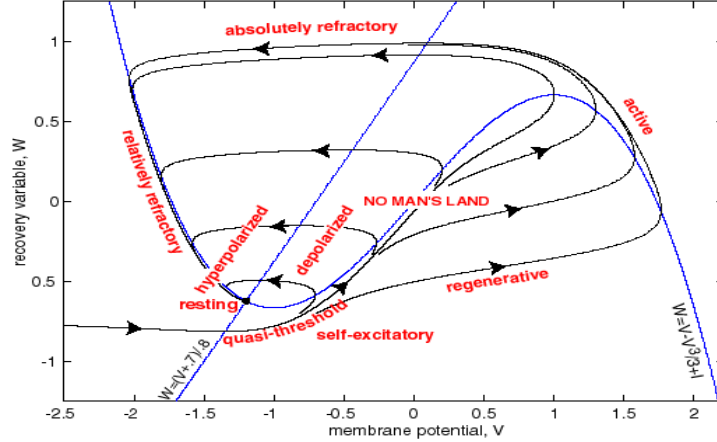


Figure 1.2: Phase portrait of FitzHugh-Nagumo neuron showing the different dynamical states.

1.3 Hindmarsh-Rose Neuron model

Hindmarsh and Rose proposed a new model in 1984, for explaining the bursting dynamics of a neuron present in the brain of *Lymanaea*, a type of pond snail. This model is computationally simple and is also capable of replicating the behaviour of biological neurons. As demonstrated in their paper in 1984, it is fairly successful in replicating the bursting activity in molluscan neurons. The equations of motion of HR neuron is given by:

$$\dot{x} = y - ax^3 + bx^2 - z + I_e \tag{1.3.1}$$

$$\dot{y} = c - dx^2 - y \tag{1.3.2}$$

$$\dot{z} = \epsilon(s(x - x_r) - z) \tag{1.3.3}$$

In these equations, the variable x represents the membrane potential, y represent the recovery variable similar to the variables v and w in FHN neuron model. However y nullcline is a nonlinear function. The variable z is a slow adapting variable, representing the slow hyperpolarizing current. The fast and slow subsystems interact to give the bursting behaviour of x . The parameters c, d, s, x_r are constants where $c = 1, d = 5, s = 4$ and $x_r = \frac{-8}{5}$. We have an internal delay parameter given by ϵ which is usually taken to be $\ll 1$. Parameters a, b , internal delay ϵ and the external input current I are the control parameters of the system.

Hindmarsh-Rose (HR) neurons show rich dynamical behaviour which makes them an

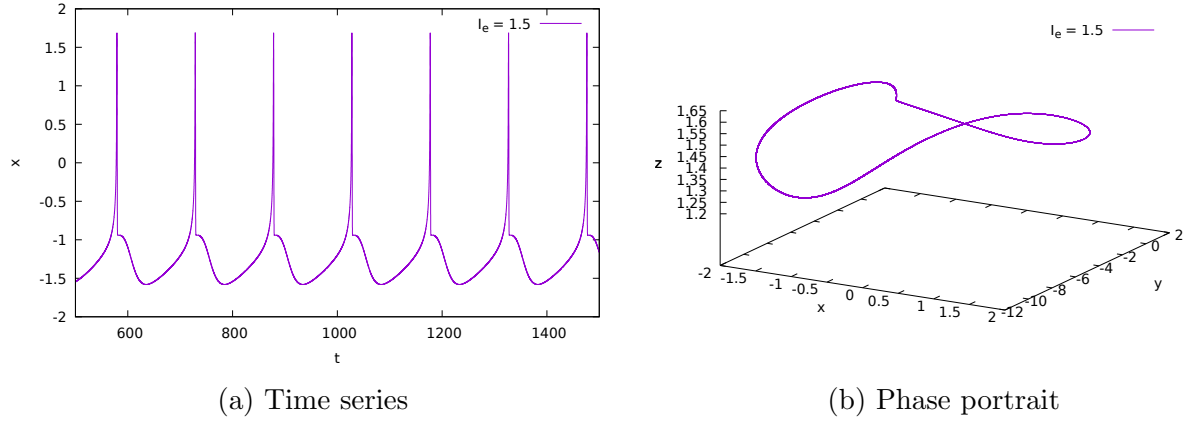
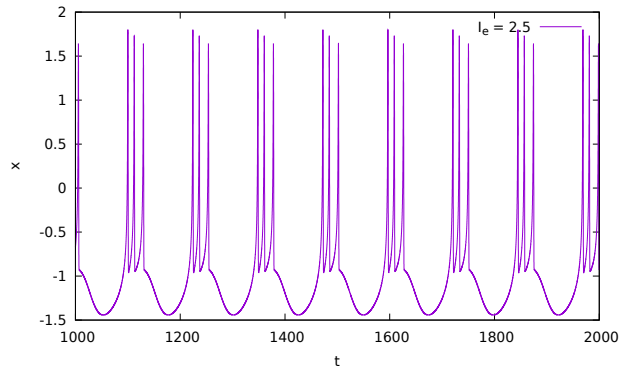


Figure 1.3: $I_e = 1.5$, Spiking dynamics

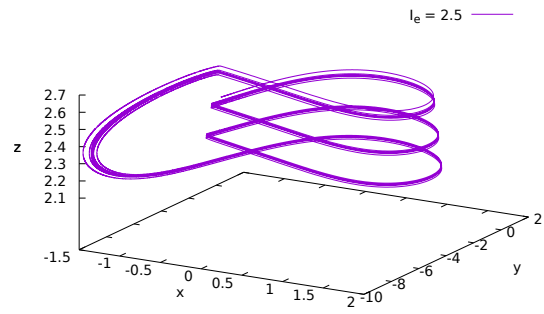
ideal system for studying dynamics of neuronal networks. There has been a lot of work following this, which showed the possible behaviours observed in the HR neurons. A very broad classification of these dynamical states are as follows [8] [9] [10] -

- *Quiescence* : Stationary state of the neuron below the threshold input.
- *Tonic Spiking* : Continuous spiking with a constant inter-spike interval.
- *Regular Bursts* : Short series of high frequency spikes which occur together in time at regular intervals.
- *Chaotic Spiking* : Continuous spiking with irregular inter-spike intervals.
- *Chaotic Bursting* : Bursting at irregular intervals or with varying number of spikes in between each burst.

Figures 1.3 - 1.7 show the different spiking and bursting dynamics of the neurons for the parameters, $b = 3$ and $\epsilon = 0.006$. But the most unique property of this neuron is bursting behaviour. Some of these bursting behaviours are demonstrated in figures 1.4 - 1.7. We also show the broad classification of the bursting states in the parameter space plot in figure 1.8.

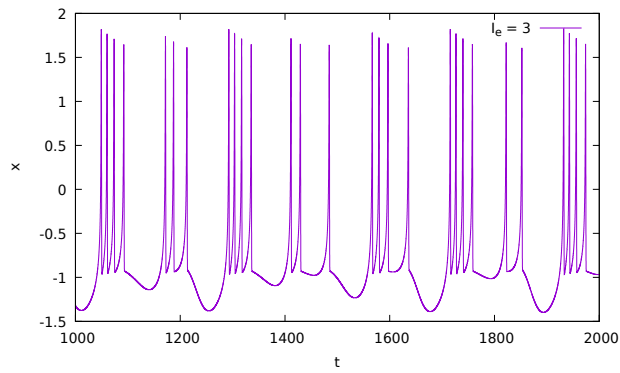


(a) Time series

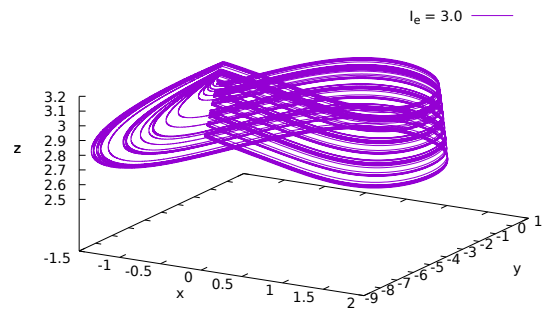


(b) Phase portrait

Figure 1.4: $I_e = 2.5$, Regular square bursts

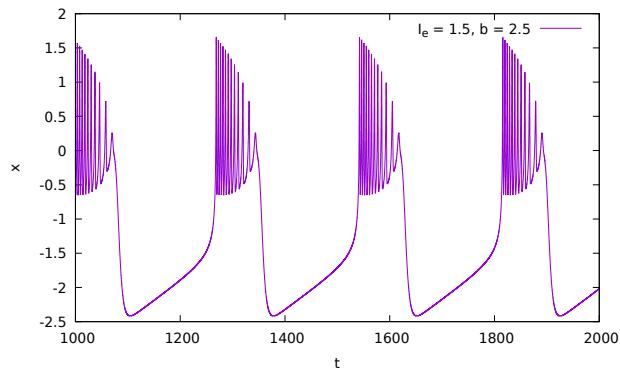


(a) Time series

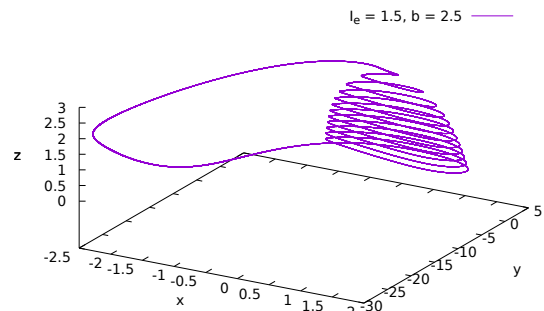


(b) Phase portrait

Figure 1.5: $I_e = 3.0$, Chaotic bursts



(a) Time series



(b) Phase portrait

Figure 1.6: $I_e = 1.5, b = 2.5$, Plateau like bursts - 1

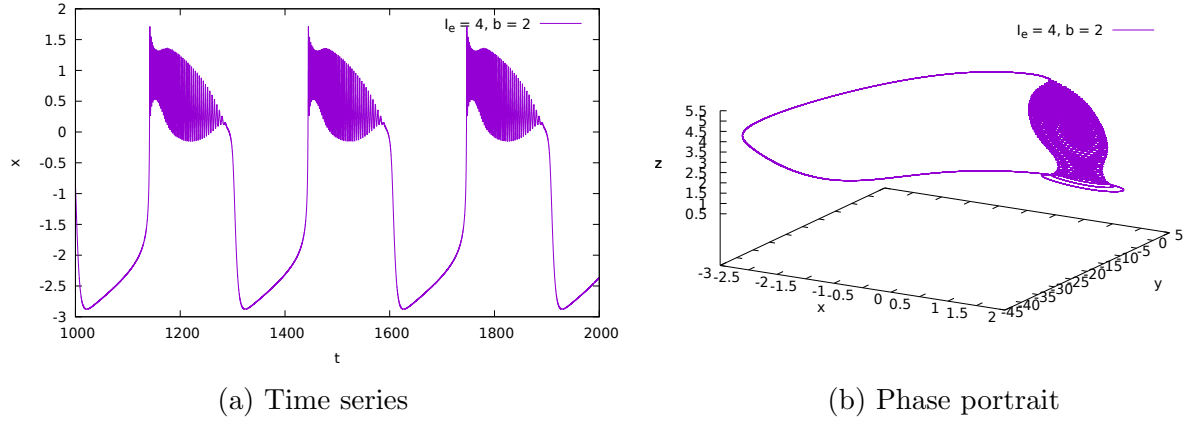


Figure 1.7: $I_e = 4, b = 2$ Plateau like bursts - 2

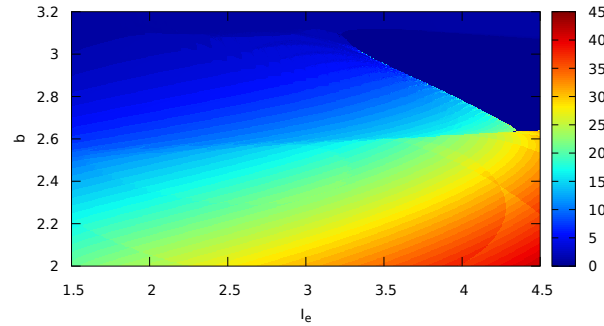


Figure 1.8: Parameter plane $I_e - b$ showing the various bursting states of the HR neurons. The colour code on the right represents the average number of spikes in between each bursts. Dark blue region corresponds to fixed points or spiking, Blue region corresponds to square bursting, light blue, yellow and orange region to plateau like bursting and red region corresponds to a region of continuous high frequency bursts.

1.4 Coupling in Neurons

Neuronal cells may individually show a variety of different behaviours as shown in the previous section, but they cannot still produce the complex behaviour of the brain or nervous system. This complicated behaviour is achieved only through the collective dynamics of the neuronal ensembles consisting of similar or different types of neurons connected via *synapses*. Synapses are like small gaps between the axon of one neuron called presynaptic neuron and the dendrites of the next one called the postsynaptic neuron.

Neurons talk to each other through these synapses and their language of communication

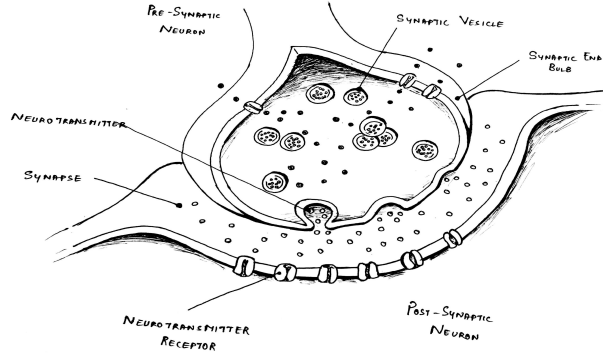


Figure 1.9: Schematic diagram of a synaptic transmission

is the neurotransmitters. When an action potential reaches the axon terminal of the presynaptic neuron they activate the Ca^{2+} ion channels which in turn release neurotransmitters into the synaptic cleft between the two neurons. These neurotransmitters bind to the receptors present in the dendrites of the postsynaptic neurons which causes action potentials. Schematic diagram of the synaptic transmission is shown in figure 1.9.

There are two different types of coupling in neurons given as:

- *Electrical Coupling* - linear coupling, which usually occurs in neuromuscular junctions. Electrical coupling is given as,

$$\Gamma(x_i, x_j) = x_j - x_i \quad (1.4.1)$$

- *Synaptic Coupling* - nonlinear coupling, which is present in brain and spinal cord.

In our models we mostly focus on the nonlinear synaptic coupling, as it is more widely present in the biological neuronal networks [11]. However we do talk about the effect of linear coupling in the neurons for certain cases. There are several ways to model the synaptic coupling, some examples being - pulse-coupling using the Θ -function, sine or cosine coupling or sigmoidal coupling. We use a sigmoidal coupling function as it is an apt model for synaptic transmission given as -

$$\Gamma(x_i, x_j) = \frac{V - x_i}{1 + e^{-\lambda(x_j - K)}} \quad (1.4.2)$$

Here the parameter V represents the reversal potential, that decides whether the synapse is excitatory or inhibitory, λ is the slope of the sigmoidal curve and K is the threshold of spiking of the sigmoid. The typical values of the coupling parameters used in our simulation are given as $V = 2$, $\lambda = 1$ and $K = -0.25$. Biologically this means that when the membrane potential of the pre-synaptic neuron is higher than -0.25 units then there is neurotransmitter release which gives an input $\Gamma(x_{post-synaptic}, x_{pre-synaptic})$ in the post-synaptic neuron. The figure 1.10 shows the form of the function Γ at these paramters.

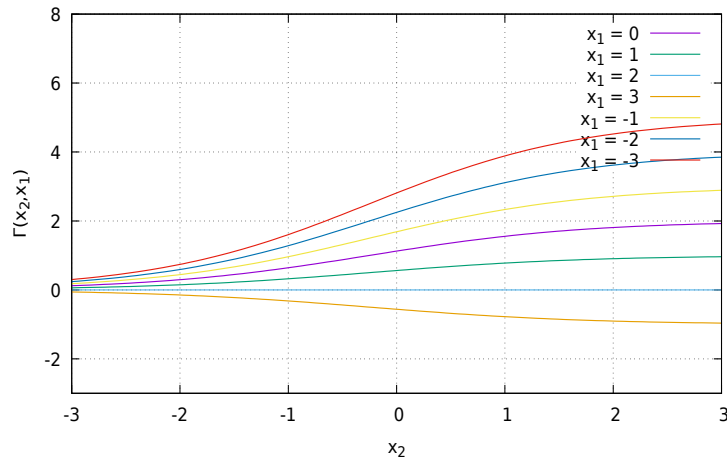
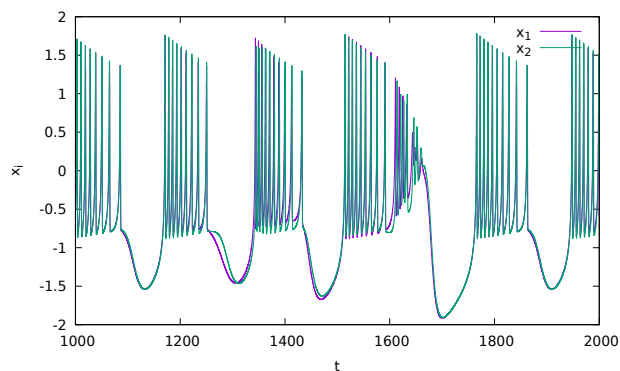


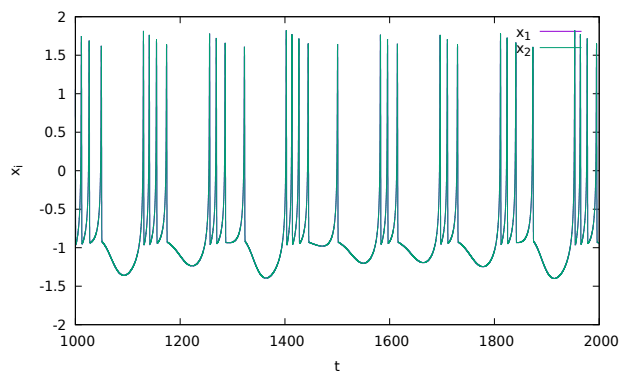
Figure 1.10: Synaptic coupling function Γ plotted for different values of x_1 and x_2 .

Coupling can result in synchronization of neuronal oscillators. In the case of HR neurons irrespective of the individual dynamics, stronger coupling strength leads to synchronization. In case of linear electrical coupling we see complete synchronisation of the neuronal oscillators whereas in case of synaptically coupled neurons, there is no complete synchronization but bursting phases of the neurons are synchronized.

Also we observe that at a certain threshold value of the coupling strength i.e. $g_{th} \sim 2$ the neurons go to a stable limit cycle of very low amplitude oscillations. If $g_s > g_{th}$, it results in complete oscillation death or amplitude death. This is shown in figure 1.12.

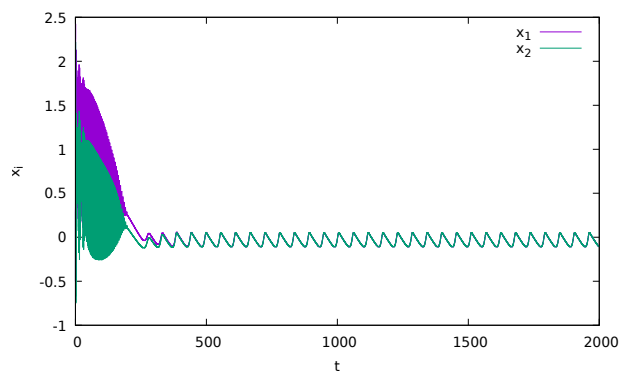


(a) Synaptic coupling. $g_s = 0.5$

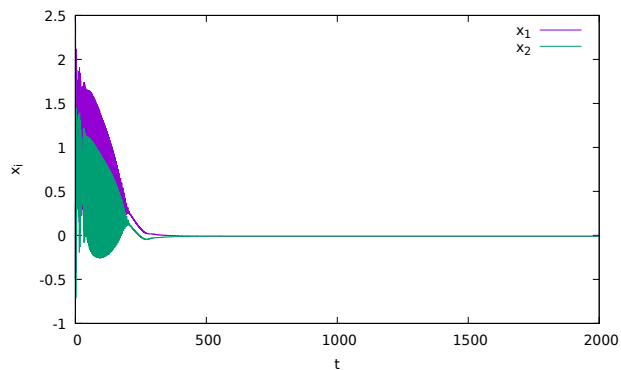


(b) Electrical coupling. $g_s = 0.5$

Figure 1.11: Synchronization in two mutually coupled chaotically bursting HR neurons. We see that at same value of g_s the electrically coupled neurons are completely synchronized whereas the synaptically coupled neurons are in phase synchronization.



(a) Low amplitude oscillations before the onset of amplitude death at $g_s = 2$ for synaptically coupled chaotic burstic HR neurons



(b) Electrical coupling. $g_s = 0.5$

Figure 1.12: Amplitude death at $g_s > 2$ for synaptically coupled chaotic bursting HR neurons.

1.5 Outline of Study

We presented in this chapter a few dynamical models for neurons like - HH, FHN and HR. There are also discrete dynamical models like Rulkov model [12], that can model the action potential sequences in neurons and hence widely used for neuronal dynamics. Our subsequent studies are mostly with HR neuron model. In this chapter studies on single HR neuron showing a multitude of dynamical states are illustrated in figures 1.3 - 1.7. We also look at various effects of electrical and synaptic coupling in neurons (figures 1.11 and 1.12).

We would be exploring the effect of multiple time-scales in coupled neurons. There has been quite a lot of work done in interacting oscillators of slow and fast systems [13] and it is observed that these systems can go to a state of no oscillations called the *amplitude death* due to timescale mismatch. In case of neurons this is an interesting point to explore as the neuronal dynamics already has two internal time-scales (ϵ for example in HR neurons), and it plays a very important role in the dynamics of individual and coupled systems.[14] [15]. In this context we note that there has been a lot of work on the effect of internal delay and how it interacts with coupling delay [16].

We initially explore this concept of coupling neurons with differing time-scales in chapters 2 and 3. We consider cases of mutually coupled neurons and simple networks like a chain of neurons and quantify their dynamical behaviour. We then extend the study to the dynamics of neurons on complex networks. There are evidences of network structure like modular structure in the brain architecture [17] [18] [19]. Such neuronal networks can show very interesting dynamical behaviour like - Synchronization, Phase-synchronization, Chimera states etc. [20] [21] [22] [23] [24] [25] [26]. Our study presented in chapter 4, is on various dynamical states possible for neurons on a modular network with excitatory and inhibitory couplings. We summarize our main results and conclusions, and future prospects of study in the final chapter.

Chapter 2

Mutually Coupled Slow and Fast Neurons

In the real case of neuronal networks we rarely have neuronal networks or ensemble of exactly identical neurons rather the neurons generally have different dynamical time-scales of firing or bursting and in some cases different dynamics all together. It is these diversity in the neuronal dynamics from cell to cell and from the region to region that give rise to some of the most remarkable features observed in the brain dynamics [27]. Often in a group of identical neurons we have certain neurons which are abnormal or diseased which results in a different time-scale in their responses. In this chapter we report our study on the dynamics of mutually coupled neurons with differing time-scales.

2.1 Coupled Neurons with differing Time-scales

The intrinsic activity of a single neuron anyway involves the interplay of time-scales, for eg. in the case of HR neurons we have z as the slow adapting variable dependent on the the internal delay parameter ϵ . In our approach towards introducing time-scale differences, we make the full dynamics of a neuron evolve slowly in time compared to the other neuron. We use the equations of HR neurons in the parameter regime exhibiting chaotic square bursts i.e. $I_e = 3.0$, $b = 3.0$ and $\epsilon = 0.006$ and tonic spikes at $I_e = 1.5$ and then study the dynamics

of the coupled systems in the presence of the time-scale mismatch. Our model is given as:

$$\dot{x}_i = \eta_i(y_i - x_i^3 + 3x_i^2 - z_i + I_e + g_s\Gamma(x_i, x_j)) \quad (2.1.1)$$

$$\dot{y}_i = \eta_i(1 - 5x_i^2 - y_i) \quad (2.1.2)$$

$$\dot{z}_i = \eta_i(0.006(4(x_i + 1.6) - z_i)) \quad (2.1.3)$$

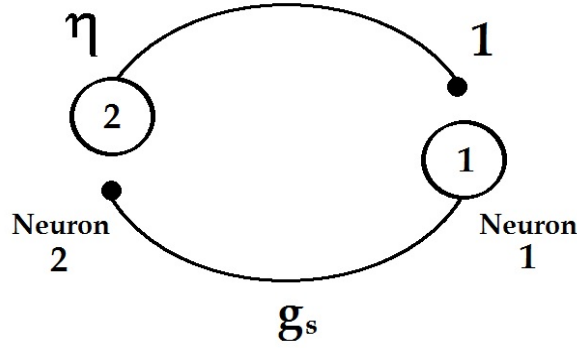


Figure 2.1: Mutually coupled neurons

Now in this model we essentially retain all the parameters in equation from the HR neuron model given in equation 1.3.1-1.3.3 and introduce a parameter η_i which gives the dynamical time-scale of the neurons. Here the parameter g_s is the coupling strength of the coupled neurons. For the case of two mutually coupled neurons we take $\eta_1 = 1$ and $\eta_2 = \eta$ so that η represents the mismatch in time-scale between the neurons. Thus we introduce time-scale mismatch in the identically coupled neurons so that one becomes slower with respect to the other one with $\eta \in (0, 1)$. The equations of motion are then:

$$\dot{x}_1 = y_1 - x_1^3 + 3x_1^2 - z_1 + I_e + g_s\Gamma(x_1, x_2) \quad (2.1.4)$$

$$\dot{y}_2 = 1 - 5x_1^2 - y_1 \quad (2.1.5)$$

$$\dot{z}_3 = 0.006(4(x_1 + 1.6) - z_1) \quad (2.1.6)$$

$$\dot{x}_2 = \eta(y_2 - x_2^3 + 3x_2^2 - z_2 + I_e + g_s\Gamma(x_2, x_1)) \quad (2.1.7)$$

$$\dot{y}_2 = \eta(1 - 5x_2^2 - y_2) \quad (2.1.8)$$

$$\dot{z}_2 = \eta(0.006(4(x_2 + 1.6) - z_2)) \quad (2.1.9)$$

We analyse the dynamics of this equation in the subsequent section.

2.2 Calculation of Burst Frequency

Calculating the frequency of the neurons is the major challenge encountered as the system at hand has several internal and external time-scales involved. Differing time-scales in this system leads to low frequency bursting dynamics and a high frequency spiking dynamics. Further adding to this is the fact that the dynamics of the neurons is mostly chaotic or irregular. So we focus the attention to only bursting dynamics of the neurons and calculate the average frequency of the bursts.

To calculate the burst frequency, we first integrate the whole system using 4th order Runge-Kutta algorithm for around $\sim 4 \times 10^5$ times, at an integration step of $\Delta t = 0.01$ and remove the transients. We save the remaining time series of the membrane potential x_i for both the neurons. Then we count the number of the times the membrane potential i.e. the variable x_i hits a global minima of a cycle of burst, occurring at all $x_i < -1.25$. The time at each point of the minima is recorded as τ^k . The Inter-burst interval (IBI) is then calculated for each burst as the time interval $\Delta\tau^k = \tau^{k+1} - \tau^k$.

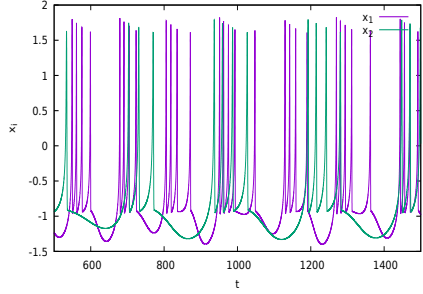
The average burst frequency of the i^{th} neuron is given by:

$$\omega_i = \frac{2\pi}{K_i} \sum_{k=1}^{K_i} \frac{1}{\tau_i^{k+1} - \tau_i^k} \quad (2.2.1)$$

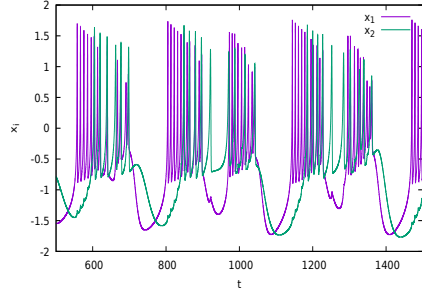
where K_i is the number of bursts in the total time used in calculation and the phase of the i^{th} neuron is given as:

$$\phi_i(t) = 2\pi \left(k + \frac{t - \tau_i^k}{\tau_i^{k+1} - \tau_i^k} \right) \quad (2.2.2)$$

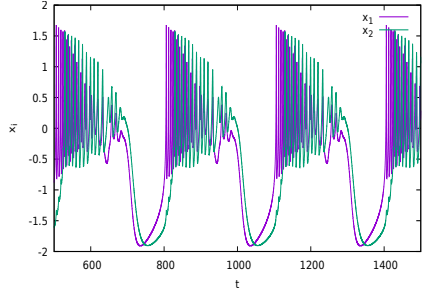
However there are certain errors possible in counting of the burst in case of irregular spiking or bursting. Hence we take a possible window T , such that the neuron activity is considered as a burst only if $\Delta\tau > T$. The value of T is decided after examining the time-series at various parameters of g_s and η . For the typical case of regular square bursting neurons, we take $T \simeq 100$ timesteps.



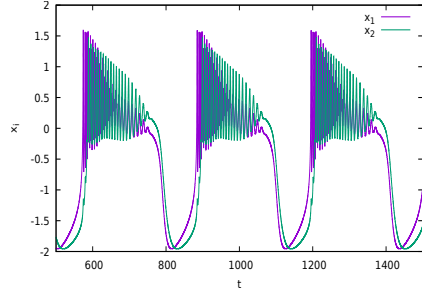
(a) $g_s = 0$ and $\eta = 0.5$



(b) $g = 0.5$ and $\eta = 0.5$



(c) $g = 1.0$ and $\eta = 0.5$



(d) $g = 1.5$ and $\eta = 0.5$

Figure 2.2: Time-series of x_i . Increasing the coupling strength from (a-d) for a constant η we find the systems tending towards a frequency synchronized state. But there is no state of complete synchronization for them.

2.3 Dynamics of Coupled Slow and Fast Neurons

Involving two different time-scales for HR neurons obviously prevents them from synchronizing. Looking at the time series of the neurons at different values of η and g_s , we find that the two neurons end up with similar bursting behaviours at higher coupling even if the two systems are not in synchrony. This is shown in the time series of x_i of the neurons in figure 2.2. We also look at the phases of the two neurons, and find that the phase of the two are also not synchronized in most cases. This leads to looking at the bursting frequency of the neurons. Now in the case of neurons this is a very relevant way of quantifying their behaviour as information in neuronal signals is mostly coded in the form of the rate of firing of the action potentials.

The emergent dynamics of the two coupled neurons with the time-scale mismatch is captured on an $\eta - g_s$ parameter plane. We broadly classify the possible dynamical states of the system as:

- Frequency Desynchronized (FD) Region (Red)
- Frequency Synchronized (FS) Region (Green)
- Amplitude Death (Blue)

These regions are shown in the figure 2.3 and 2.4 with the colour code given above.

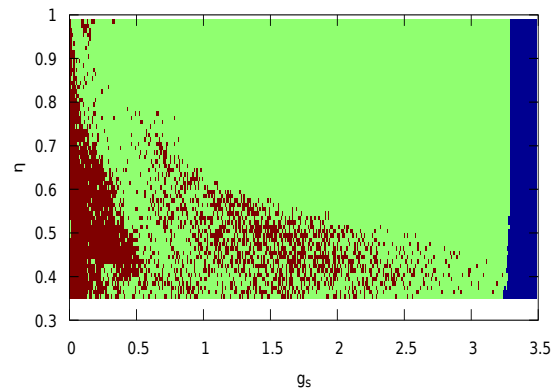


Figure 2.3: Regions of frequency synchronization for spiking neuron at $I_e = 1.5$. **Red region** corresponds to **FD**, **Green region** corresponds to **FS** and **Blue region** corresponds to **AD**.

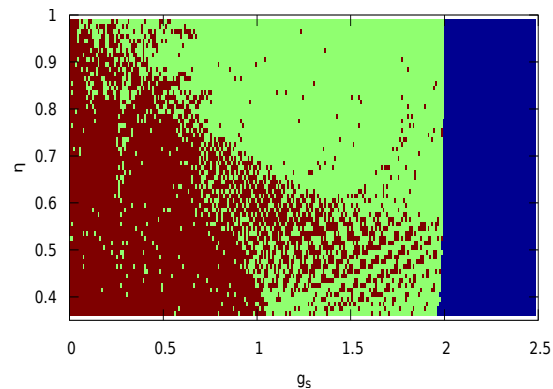


Figure 2.4: Regions of frequency synchronization for chaotic bursting neuron at $I_e = 3$. **Red region** corresponds to **FD**, **Green region** corresponds to **FS** and **Blue region** corresponds to **AD**. We observe a broader region of FD as the intrinsic dynamics is chaotic to begin with.

Now we see a basic trend in the plots 2.3 and 2.4 that as the coupling strength increases the synchronized green region increases. However as the time-scale mismatch is higher i.e.

η decreases, this region disappears. This basically points out the fact that the parameter η breaks the symmetry between the two otherwise identical systems.

An interesting result that we observe is that as discussed in Section 1.5, in the case of generic oscillatory systems, interaction of slow and fast systems may lead to amplitude death. But in the case of neurons, we observe that there is no amplitude death due to time-scale mismatch. Rather it is observed that both the neurons still go to a state of amplitude death when $g_s > 2$ for chaotic bursting neurons and $g_s > 3.25$ for tonic spiking neurons, irrespective of the difference of time-scale between them.

We note that amplitude death at high coupling strength is a consequence of the nonlinear nature of the coupling in neurons. We verify this by looking at a similar $\eta - g_s$ parameter plane for electrically coupled neurons in figure 2.5. Here there is no amplitude death even at very high coupling strengths. We propose that this is because in case of synaptic coupling beyond a certain value of g_s , the value of Γ is too high for the post-synaptic neuron to recover. Hence the limit cycle behaviour is reduced to a stable fixed point.

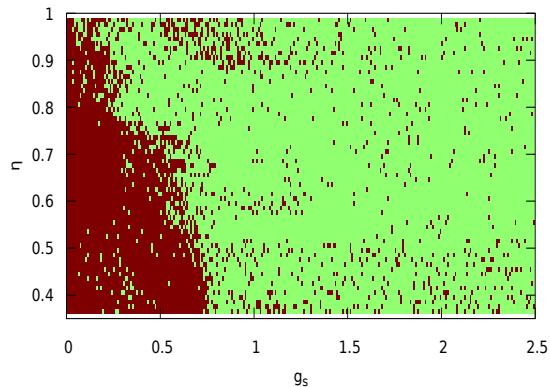


Figure 2.5: Regions of frequency synchronization for chaotic bursting neurons at $I_e = 3$ coupled electrically. We observe an absence of AD in this case. This shows that nonlinear coupling causes AD in neurons, not timescale mismatch.

Now we concentrate on the FS region, and study possible frequency patterns we can get for the different values of η and g_s . For this we plot the average frequency of the two slow and fast systems in the FS region. The figures 2.6 and 2.7 show the different frequencies present in the system with the colour code as indicated. We find that there is a suppression of the natural frequency of the neurons. Interacting slow and fast neurons make the system

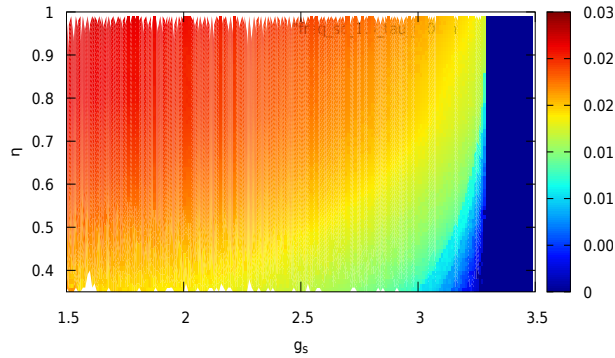


Figure 2.6: Frequency suppression in regularly spiking neurons, $I_e = 1.5$

to settle to an emergent frequency which is much less than the average intrinsic frequencies of the neurons. The pattern of suppression of the emergent frequency is similar for spiking and chaotic bursting neurons.

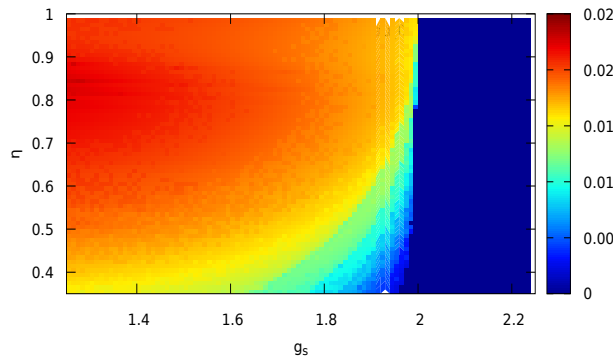


Figure 2.7: Frequency suppression in chaotic bursting neurons, $I_e = 3$

In this context we note that, frequency suppression is also reported in case of other non-excitable oscillators [13]. From the point of view of neurons this is a very interesting result since the frequency of the emergent state can be controlled by varying the values of the nonlinear coupling strength and time-scale mismatch. It is possible that interaction of a network of neurons with differing time-scales may lead to an emergent dynamical state with suppressed frequency. We therefore extend this model to certain simple networks like a directed chain of synaptically coupled neurons with each one having a different time-scale. The following chapter reports our study on the dynamics of such systems.

Chapter 3

Dynamics of HR Neurons on Regular Networks

In the previous chapter, we report the dynamics of mutually coupled slow and fast neurons. We observe that in such a system of neurons with different time-scales instead of achieving complete synchronization, the system becomes frequency synchronized with emergent frequency much less than the average intrinsic frequencies of the HR neurons. Now we extend this to a system, where the neurons are coupled in regular networks.

3.1 Ring of HR neurons

We begin with the simplest of such networks of HR neurons - a linear chain with a periodic boundary conditions shown in figure 3.1. We introduce time-scale mismatch by making each neuron slower than the previous one by some $\Delta\eta$. Our model is given as:

$$\dot{x}_i = \eta_i(y_i - x_i^3 + 3x_i^2 - z_i + I_e + g_s(2 - x_i) \sum_{j=1}^N a_{ij}\Gamma(x_j)) \quad (3.1.1)$$

$$\dot{y}_i = \eta_i(1 - 5x_i^2 - y_i) \quad (3.1.2)$$

$$\dot{z}_i = \eta_i(0.006(4(x_i + 1.6) - z_i)) \quad (3.1.3)$$

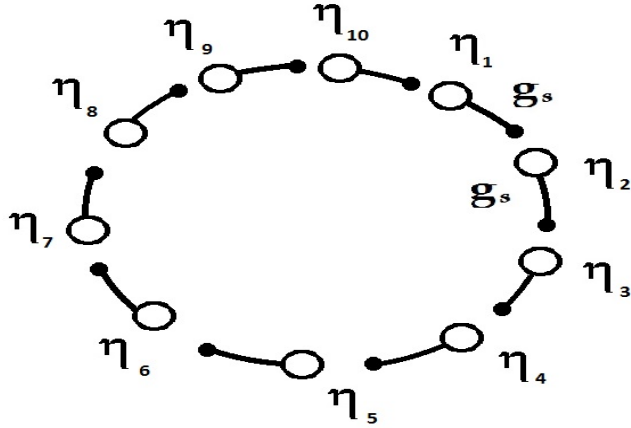


Figure 3.1: Ring of neurons with differing time-scales

Here $i = 1, 2, 3, \dots, N$ index refers the number of neurons in the ring. We restrict the intrinsic dynamics in this model to only the chaotically bursting neurons, hence $I_e = 3$ in all cases.

The parameter a_{ij} represents the ij^{th} element of the adjacency matrix A that uniquely represents the network configuration where:

$$a_{ij} = \begin{cases} 1 & , \text{ if node } i \text{ and } j \text{ are connected} \\ 0 & , \text{ if they are disconnected} \end{cases}$$

in the case of unweighted networks. The diagonal elements of the adjacency matrix are 0 as there are no self couplings. The matrix A is symmetric when the connections are unidirectional i.e. if i and j nodes are coupled then the vice-versa is also true. For a directed network the matrix is asymmetric.

In our model with neurons we make the network directed as the interaction at a synapse of a neuron is unidirectional, from presynaptic neuron to the postsynaptic one. In this network every neuron essentially receives input from only one neuron and passes on its input to the next one. So essentially this system would reduce to the previous one if we have $N = 2$. The

adjacency matrix for such a ring of neurons shown in figure 3.1 is given by -

$$A = \begin{pmatrix} 0 & 0 & 0 & 0 & 0 & 0 & 0 & 0 & 0 & 1 \\ 1 & 0 & 0 & 0 & 0 & 0 & 0 & 0 & 0 & 0 \\ 0 & 1 & 0 & 0 & 0 & 0 & 0 & 0 & 0 & 0 \\ 0 & 0 & 1 & 0 & 0 & 0 & 0 & 0 & 0 & 0 \\ 0 & 0 & 0 & 1 & 0 & 0 & 0 & 0 & 0 & 0 \\ 0 & 0 & 0 & 0 & 1 & 0 & 0 & 0 & 0 & 0 \\ 0 & 0 & 0 & 0 & 0 & 1 & 0 & 0 & 0 & 0 \\ 0 & 0 & 0 & 0 & 0 & 0 & 1 & 0 & 0 & 0 \\ 0 & 0 & 0 & 0 & 0 & 0 & 0 & 1 & 0 & 0 \\ 0 & 0 & 0 & 0 & 0 & 0 & 0 & 0 & 1 & 0 \end{pmatrix} \quad (3.1.4)$$

The coupling function Γ is the synaptic coupling function of the form $\Gamma(x_j) = (1 + e^{-(x_j+0.25)})^{-1}$. Typical size of the rings considered are $N = 30$ and $N = 40$.

3.2 Dynamics of Neurons on a Ring

The slowness parameter η varies for successive neurons in the ring as:

$$\eta_{i+1} = \eta_i - \Delta\eta \quad (3.2.1)$$

We take $\Delta\eta = 0.02$ and $\eta_1 = 1$ for all cases such that $\eta_{30} = 0.4$ and $\eta_{40} = 0.2$, which is significantly lower than η_1 . We look at the spatial plot of the neuron burst frequency to capture the difference in the time-scales between the neurons and find that the frequency of the neurons is linearly related in absence of coupling as shown in figure 3.2.

We consider two different values of the total number of neurons $N = 30$ and 40 and we find qualitatively similar dynamics in both these cases. For weak coupling strength, we observe that the neurons enter into frequency synchronized clusters with frequencies lower than the average of the intrinsic value. This is clear from the colour coded patches of different frequencies shown in fig 3.3.

The number of these clusters reduces as we gradually increase the coupling strength.

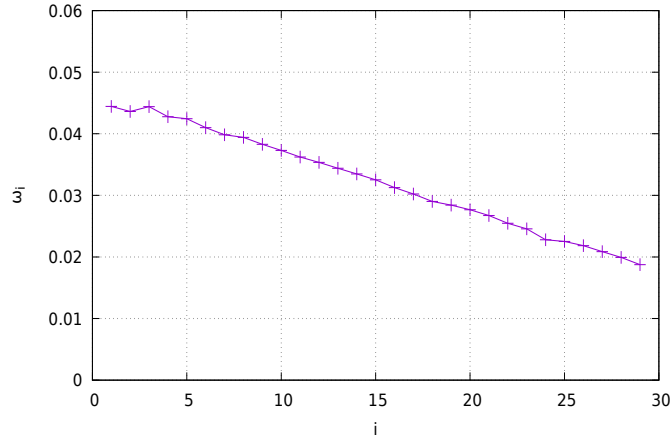


Figure 3.2: Frequency of each isolated neuron when $g_s = 0$ and $\Delta\eta = 0.02$.

Finally at a certain coupling strength $g_s = 0.75$, they tend to collapse into a single cluster of *Synchronized Frequency Supressed State (SFSS)*, with a frequency less than half of the intrinsic frequency of the HR neurons.

We repeat the above study for $N = 100$ neurons with $\Delta\eta = 0.005$ and the results are shown in figure 3.4. In this case, we see that the burst frequency instead of forming distinct coloured bands of frequency clusters, gradually decreases on the ring as the neurons become slower and slower. We therefore conclude that the formation of frequency clusters at lower g_s depends on the step size of mismatch in time-scale, $\Delta\eta$.

3.3 Summary

Based on the results of the study presented in this chapter and previous one, we can summarize the main conclusions as:

1. Unlike the case of general coupled oscillators, where time-scale mismatch can lead to an amplitude death (AD) state, coupled neuronal systems with differing time-scales do not go into an AD. Amplitude death occurs only in the case of synaptically coupled neurons at very high values of coupling strength. This phenomenon is interesting in a way as it shows the fundamental difference in the way neurons or other excitable systems behave compared to other oscillating systems like Rossler, Lorenz or Duffing

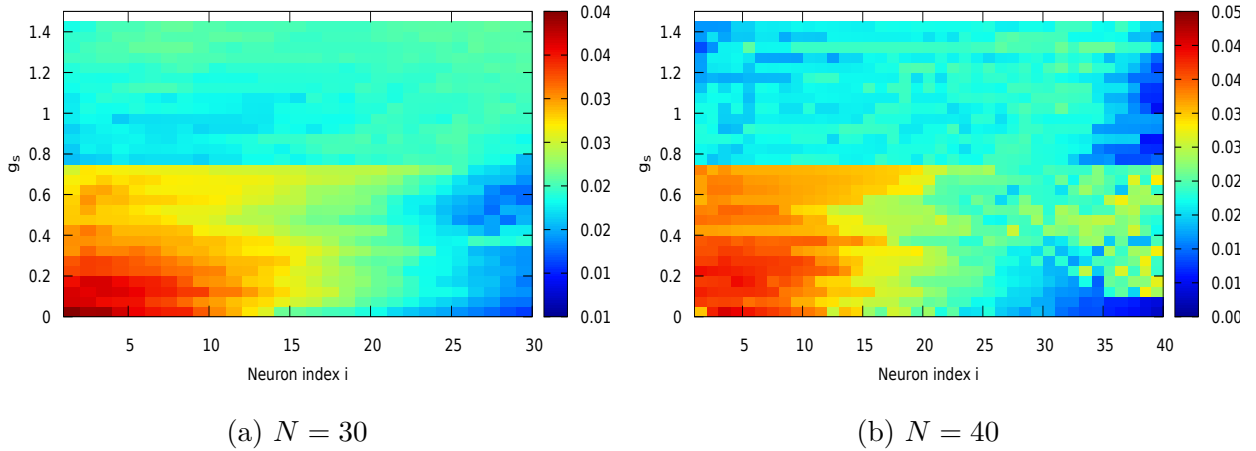


Figure 3.3: Frequency suppressed clusters for a ring of neurons with increasing coupling strength. In both these cases, there are clusters of frequency synchronized neurons which finally collapse into a single cluster of SFSS as the coupling strength increases.

oscillators. This may be one of the major factors which make them efficient information processing units in our brain.

2. Multiple time-scales along with synaptic coupling in neurons on a ring, makes the system go into a state of Frequency Synchronized Clusters. The emergent bursting frequencies are much lower than the average intrinsic frequency of the neurons. At stronger coupling the neurons settle into a single cluster of Synchronized Frequency Supressed State. This is highly relevant in case of the neurons as neurons encode information in the form of their bursting or spiking frequencies.

The system of neurons on a ring is essentially a mathematical abstraction of real network of neurons. However we note that Medial Entorhinal Cortex (MEC) located in the temporal lobe of the mammalian brain does have similarly connected chain of bursting neurons with varying time-scales [28] [29]. This is the region which is responsible for spatial navigation and memory formation. Therefore the present study can be a prospective model to understand the topology and dynamics of these neurons.

These interesting results encourage us to persue the study on more realistic networks of neurons. We extend our model to a more realistic model of neuronal networks like a *Modular Networks* rather than a simple random network. In the following chapter we look at the dynamics of neurons on modular networks. We also introduce two different types of

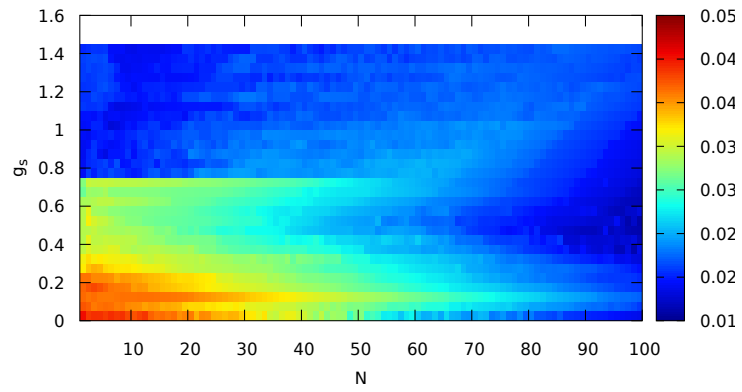


Figure 3.4: Frequency suppressed state for a ring of 100 neurons with $\Delta\eta = 0.005$. There are no distinct clusters present, the system has a continuous transition in frequency

couplings - excitatory and inhibitory, and study the dynamics of such neuronal networks.

Chapter 4

Modular Networks of HR Neurons

As given in the section 1.5, the framework of complex networks provides us with a very powerful tool for modelling the brain dynamics. In the previous chapter, we report the dynamics of regular networks of neurons. However in the real case, the neuronal networks in the nervous system of even the most simple multicellular organisms form very complicated networks. This motivates us to study the dynamics of complex networks of neurons [30] [21].

Modular network (MN) is perhaps one of the possible ways of modelling the neuronal networks in the brain and spinal cord. They form one of the possible networks which give rise to a community like structure in networks. Such community structured networks are very common in the mammalian brain and in the nervous systems of animals [17] [31]. There have been some recent studies on the dynamics of neuronal networks with a modular structure and interesting results like chimera-like states and patterns of synchronizations etc reported [19] [32] [18] [33]. We also consider inhibitory coupling which is very crucial in neuronal dynamics in the brain [32] [34] [35].

In this chapter, we report our study on specific models on neuronal networks with modular structure including an inter-play between excitatory and inhibitory coupling.

4.1 Generating Modular Networks

One of the simple ways of generating a network with community structure is the *Stochastic Block Model* [36]. We start with a random network with N nodes. We group these nodes into M different communities or modules. The nodes inside a community have a different average degree than the inter-community degree. So we define a *Stochastic Block Matrix (SBM)* Ω of dimensions $M \times M$ whose element ω_{lk} denotes the probability of forming an edge between the two nodes in module l and k ($l, k = 1, 2, 3 \dots M$).

For generating the adjacency matrix of a network, we simply go to each node i and j and then draw a random number from a uniform distribution between 0 and 1, r . Now we identify the module in which i and j belong to respectively. Suppose $i \in l$ and $j \in k$, we then compare the random number obtained for each pair of node to their respective element of Ω . Now if $r \leq \omega_{lk}$ then the respective $a_{ij} = 1$ i.e. a connection is present between the two nodes, otherwise not.

So the distribution of edges is independent but non identical to each other. This depends on the module in which the two nodes belong, making them conditionally independent. Based on how we group the nodes and the matrix Ω we can create networks of various topology. For example:

- if $\omega_{ij} = \omega$ for all i, j , we get an Erdos-Renyi network.
- if $\omega_{ij} < \omega_{ii}$ for $i \neq j$, we get an assortative network. Here the edges between similar nodes have a higher degree, hence we can see the communities densely connected among each other and sparse connections between communities.
- if $\omega_{ij} > \omega_{ii}$ for $i \neq j$, we get disassortative networks i.e. the similar type of nodes have a lower degree of connections.

In our study, we will consider the two different cases - assortative and disassortative neuronal networks. The brain usually consists of several clusters of identical (structurally or functionally) neurons, which essentially represents a module. Such clusters of structurally and functionally identical neurons in the Central Nervous System are called nucleus. Now we can form different such networks with several modules forming assortative and disassortative networks based on the SBM.

4.2 Modular Neuronal Networks

We consider a network of $N = 100$ neurons, divided into $M = 4$ modules. Therefore each module has exactly 25 neurons. The equations of motion of HR neurons in this context are given as:

$$\dot{x}_i = \eta_i \left(y_i - x_i^3 + 3x_i^2 - z_i + I_e + g_s(2 - x_i) \sum_{i=1}^N a_{ij} \left(\frac{1}{e^{-10(x_j+0.25)}} \right) \right) \quad (4.2.1)$$

$$\dot{y}_i = \eta_i(1 - 5x_i^2 - y_i) \quad (4.2.2)$$

$$\dot{z}_i = \eta_i(0.006(4(x_i + 1.6) - z_i)) \quad (4.2.3)$$

We take $I_e = 3.0$ such that the neurons are always in chaotic bursting state. g_s is represented as:

$$g_s = \begin{cases} \alpha & , \text{ for intra-module coupling strength} \\ \beta & , \text{ for inter-module coupling strength} \end{cases} \quad (4.2.4)$$

For all cases of study we have $\alpha > 0$ and $\beta < 0$ making intra-module coupling excitatory and inter-module coupling inhibitory. Here we take $\eta_i = 1$ for all the neurons such that they are in the same time-scale of dynamics.

The adjacency matrix element A is generated with the help of the Stochastic Block Matrix using the algorithm mentioned in the preceding section. We make the network directed as the coupling between the neurons are directed from pre-synaptic to post-synaptic neurons. The two different cases consider are:

- Dense excitatory connections inside the module and sparse inhibitory connections between modules.

$$\Omega_1 = \begin{pmatrix} 0.4 & 0.05 & 0.05 & 0.05 \\ 0.05 & 0.4 & 0.05 & 0.05 \\ 0.05 & 0.05 & 0.4 & 0.05 \\ 0.05 & 0.05 & 0.05 & 0.4 \end{pmatrix} \quad (4.2.5)$$

This gives us a network with community structure. We term this as the *Assortative*

Excitatory Network (AEN) as there are more number of excitatory connections in the network (fig 4.1).

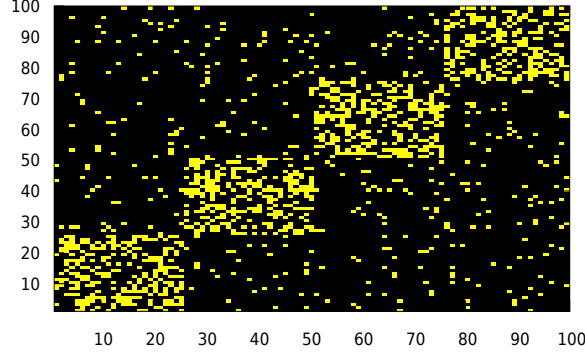


Figure 4.1: Adjacency matrix of a Associative Excitatory Network. Neurons in a module have higher number of synapses from within the module, than from outside. Hence the network has denser excitatory connections than inhibitory ones.

- Sparse excitatory connections inside a module whereas all neurons of one module are coupled to all the other neurons of other modules.

$$\Omega_2 = \begin{pmatrix} 0.05 & 1 & 1 & 1 \\ 1 & 0.05 & 1 & 1 \\ 1 & 1 & 0.05 & 1 \\ 1 & 1 & 1 & 0.05 \end{pmatrix} \quad (4.2.6)$$

We term this as the *Disassortative Inhibitory Network (DIN)* as the inhibitory connections dominate over the excitatory ones (fig 4.2).

The system is integrated using vector RK4 at step $\Delta t = 0.01$ for 500000 integrations. We remove the transients and observe the spatio-temporal plots to understand the dynamics of the system. We then develop schemes to quantify the dynamics by looking at synchronization between the various elements of the system. We also calculate the burst frequency and average burst frequency of each module, using the frequency calculation scheme presented in the previous chapters. In the following sections, we present a detailed description of the possible dynamical states in modular networks.

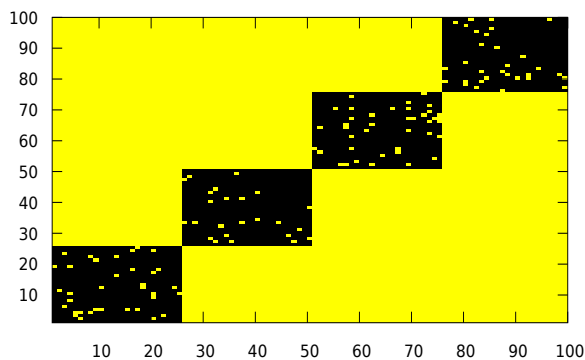


Figure 4.2: Adjacency matrix of Disassociative Inhibitory Network. All to all inhibitory connections between the modules with sparse excitatory connections.

4.3 Dynamical States in Modular Neuronal Networks

In both cases of the modular networks that we study, we observe a multitude of dynamical behaviours. This is a challenging problem in itself as there are many parameters and variables in the system. So at first we fix most of the parameters mentioned above and keep only α and β as the varying parameters of the system.

The neurons in the modules are identical, but are connected randomly. Similarly in between the modules the connections are either random as in case 1 or are all-to-all in case 2. Synapses inside the module are always excitatory whereas inter-modular synapses are inhibitory. The excitatory synaptic coupling makes the neurons phase synchronize as discussed in the chapters 1 and 2 whereas the inhibitory connections make the neurons desynchronize. So the values of the excitatory and inhibitory coupling strength α and β respectively can be tuned to give very interesting dynamical patterns of phase synchronization between the modules.

We calculate the phase of each neuron according to the equation:

$$\phi_i(t) = 2\pi \left(k + \frac{t - \tau_i^k}{\tau_i^{k+1} - \tau_i^k} \right) \quad (4.3.1)$$

where τ_i^k gives the time of onset of the k^{th} burst in the i^{th} neuron.

We check for phase synchronization in the neurons in a module using the Kuramoto order parameter. If the phases of all the N neurons are given as ϕ_i , then we can define the Kuramoto order parameter of a module as R_m such that ($i = 1, 2, 3, \dots, N$ and $m = 1, 2, \dots, M$) [21] [37]-

$$\zeta_m = R_m e^{i\Phi_m} = \frac{M}{N} \sum_{j=1}^{N/M} e^{i\phi_j} \quad (4.3.2)$$

For complete phase synchronization $R_m = 1$. If $R_m > 0.9$ then we take the modules to be in phase synchrony. Now if all the neurons in the module are all phase synchronized we can take the ensemble phase average $\langle \phi_i \rangle_m$ and consider that each module itself is bursting. The system of $N = 100$ neurons can then be reduced essentially to a system of $M = 4$ neuronal ensembles. Now we can quantify the relative dynamics of the module based on the differences in the ensemble phase average $\langle \phi_i \rangle_m$ of the neurons.

We find that we can broadly classify the dynamical states into 3 possible cases - *De-synchronized*, *Phase Synchronized* and *Activity Death*. These can be again divided into 5 substates. These 15 possible states can be listed as :

- **De-synchronized States** : Neurons burst in a desynchronized manner inside the module.
 1. State 1 - **DS-4**: Where all neurons are desynchronized
 2. State 2 - **DS-3**: One of the modules has all neurons in burst phase synchronization, but the rest of the modules are desynchronized
 3. State 3 - **DS-2**: Two of the modules have neurons in phase synchrony, rest are desynchronized.
 4. State 4 - **DS-2,P-2**: Two of the modules have neurons in phase synchrony and the phase of two modules also synchronize, whereas the rest are desynchronized.
 5. State 5 - **DS-1**: One of the module has chaotic bursting neurons, other are in burst phase synchrony
- **Phase Synchronized States** : All the neurons in a module exhibit phase synchronized bursting, which appears like the whole module is bursting.

1. State 6 - **TB**: All neurons are synchronized in phase inside each module, but the modules are all out of phase with each other. This essentially resembles a travelling burst in the networks where each module succesively burst after one another.
 2. State 7 - **PS-2**: We have two modules in phase and two modules not in phase with each other.
 3. State 8 - **PS-2,2**: We have two sets of modules in phase with other and off phase with the other.
 4. State 9 - **PS-3**: Three modules in phase and one out of phase.
 5. State 10 - **PS-4**: All neurons are in phase synchronization. This is when the whole network bursts together.
- **Activity Death States** : The neurons do not exhibit spiking or bursting dynamics, but either exhibit very low amplitude oscillations or are at a stable equilibrium point.
 1. State 11 - **AD-1**: One module stops firing.
 2. State 12 - **AD-2**: Two of the modules stop firing.
 3. State 13 - **AD-3**: Three of the modules stop firing.
 4. State 14 - **AD-4**: All the neurons stop firing and reach oscillation death.
 5. State 15 - **AD**: Neurons stop firing randomly.

We present the spatio-temporal plots for each of these states corresponding to different values of α and β . The parameter plane $\alpha - \beta$ with all the possible dynamical states of the system is also presented below.

4.4 Case 1 : Assortative Excitatory Networks

So the first case involves the network configuration based on the Stochastic Block Matrix given in equation 4.2.5. We look at the average number of synapse in this case which is basically the degree of connectivity of a certain node in the network. The average degree of connections in the modules is -

$$k_{av}^u = \omega_{ll} \left(\frac{N}{M} \right) = 10 \quad (4.4.1)$$

whereas in between the modules the average degree is -

$$k_{av}^{lk} = \omega_{lk} \left(\frac{N}{M} \right) (M - 1) = 3.75 \quad (4.4.2)$$

So every neuron can on an average have 10 excitatory synapses and 3.75 inhibitory synapses.

Some of the general trends in the dynamics that we observe are :

1. For very low values of α and high values of β , the system desynchronizes. This happens because of the random inhibitory connections between the modules that break the phase synchronization inside the modules. So we can essentially desynchronize a module by increasing the number of inhibitory synapses in the module.
2. For intermediate values of α and β , the neurons in each module phase synchronize. We therefore can see various synchronized states between the modules. The most common of these states is when two of the modules synchronize with each other and the other two are in off phase with them i.e. PS-2 and PS-2,2. We also see instances of PS-3 and TB at some values of α and β .
3. The system goes into an activity death at a much lower value of α , as the number of synapses for each neuron is higher. For $\beta = 0$, the critical value $\alpha_{th} \sim 0.35$. But inhibitory coupling can recover the system from amplitude death. Hence if $|\beta| > 0$, then $\alpha_{th} > 0.35$.
4. However for most of the values of the parameters α and β we get desynchronized dynamical states. This is mostly due to the network topology which has neurons randomly connected to each other with inhibitory and excitatory coupling.

We present spatio-temporal plots depicting the above dynamics of the network in the figures 4.3, 4.4 and 4.5. We also plot the parameter plane $\alpha - \beta$ where each coloured band is a state numbered according to the previous section.

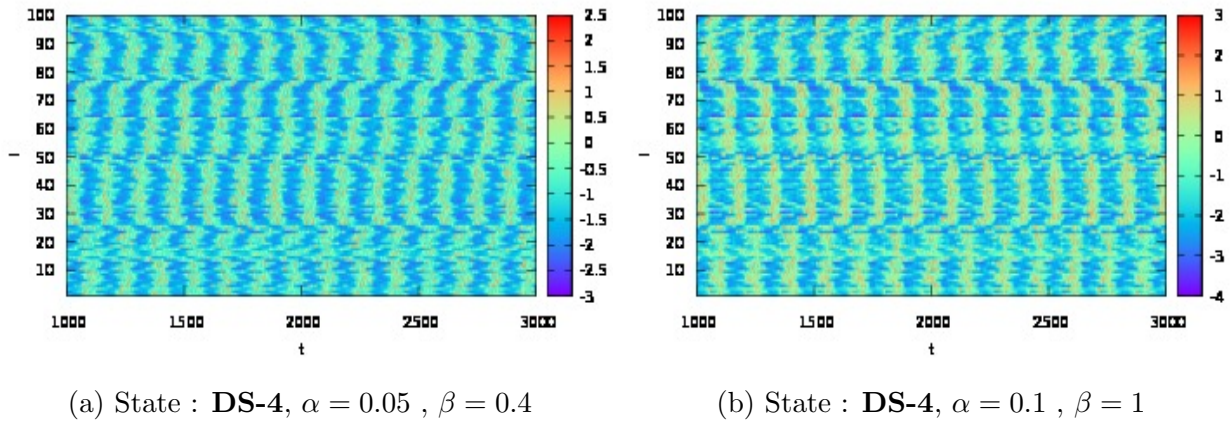


Figure 4.3: Desynchronized neurons in AEN: At very high values β the system is usually desynchronized. This is because inhibitory coupling breaks the phase synchrony between the modules

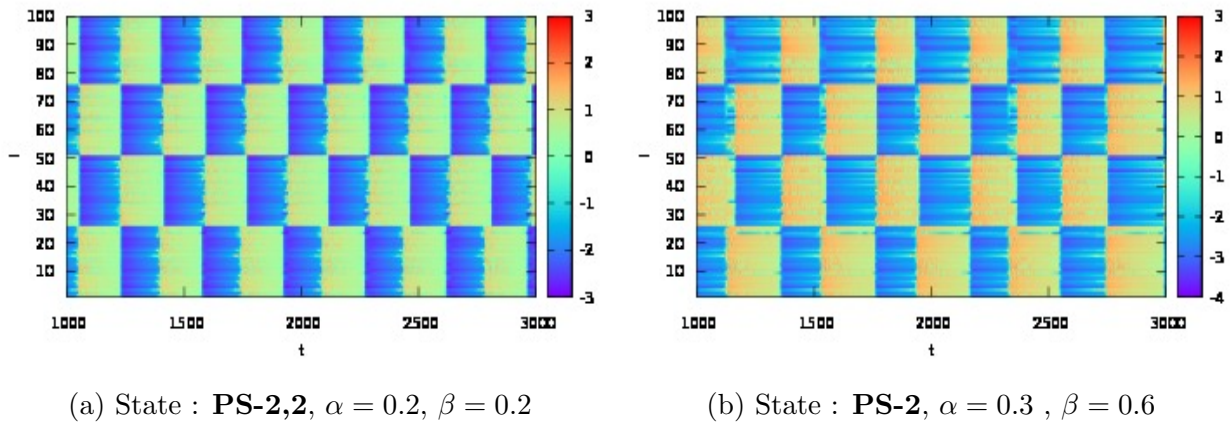
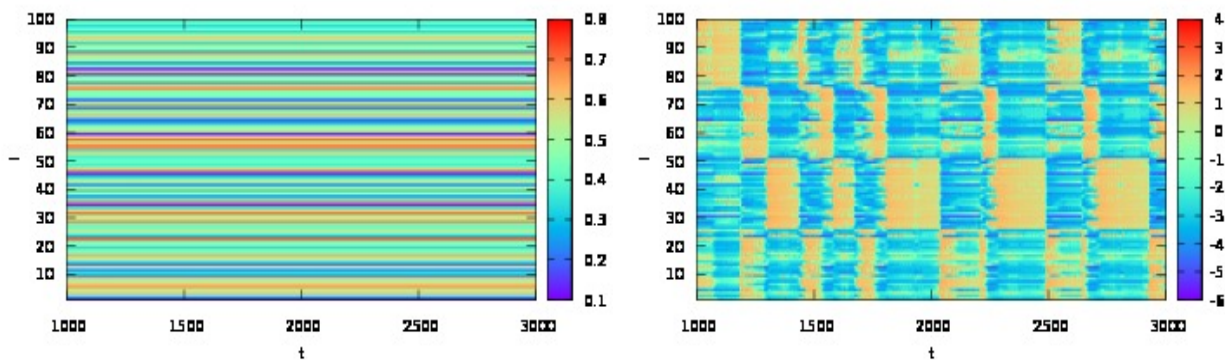


Figure 4.4: Synchronized States in AEN: At certain values of α and β we get states like these where two modules are synchronized in phase and the others are in off phase. (a) Module 1 and 2 are PS and 2 and 4 are in PS. (b) Module 1 and 3 are PS



(a) State : **AD-4**, $\alpha = 0.4$, $\beta = 0.2$

(b) State : **DS-4**, $\alpha = 0.4$, $\beta = 2$

Figure 4.5: Change in β can revive the network from AD to Desynchronized State. We increase the value of β for a constant α to force the system to burst. So essentially the inhibitory coupling can revive a system from activity death state.

4.5 Case 2 : Disassortative inhibitory Networks

This case as mentioned above is an inhibitory neuronal network. The Stochastic Block Matrix used for this case is given in equation 4.2.6. So each neuron has around 75 inhibitory synapses with other neurons whereas the average number of excitatory synapses is around 1.25.

So we summarize the general dynamical behaviour of the system as :

1. Most important dynamics in such inhibitory networks found is the travelling burst like patterns in the network. In each of the module phases of all neurons are completely synchronized, but all the modules remain in off phase with each other. This type of off phase synchronization has been observed earlier in other inhibitory networks of neurons [32]. By carefully adjusting α and β we can make the dynamics such that each module fires successively without any phase lag. This basically results in sequential bursting of each module in the system generating a travelling burst wave.
2. Tuning the parameters α and β we can alter the width of each burst. This happens solely due to the excitatory coupling in the modules. More number of excitatory connections can alter the bursting width of that module. This in the case the travelling burst, looks like it has a lag at each of the modules.

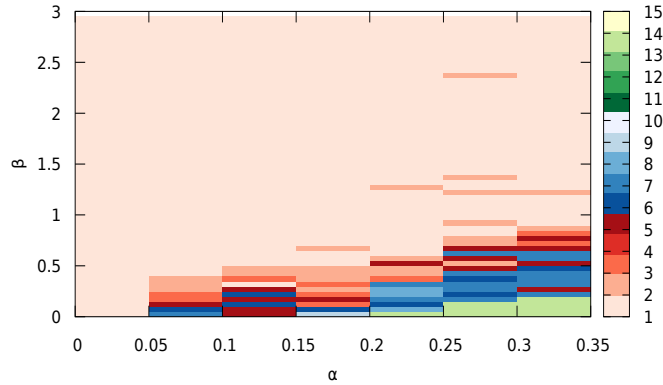


Figure 4.6: $\alpha - \beta$ parameter plane for Ω_1 . Red shades correspond to Desynchronised States, Blue shades corresponds to Phase Synchronised States, Green shades corresponds to Activity death states. The numbers given in the vertical band represent the dynamical states: 1-**DS-4**, 2-**DS-3**, 3-**DS-2**, 4-**DS-2,P-2**, 5-**DS-1**, 6-**TB**, 7-**PS-2**, 8-**PS-2,2**, 9-**PS-3**, 10-**PS-4**, 11-**AD-1**, 12-**AD-2**, 13-**AD-3**, 14-**AD-4**, 15-**AD**

3. We also observe mixed-mode oscillations (MMOs) specifically in the case of inhibitory bursting neurons (figure 4.7). MMOs are basically oscillations which consist of small amplitude and large amplitude parts. In this cases we observe regular amplitude bursts with series of small amplitude burst between them. The small amplitude burst of one module of neurons coincide with the large amplitude burst of neurons from other modules. MMOs have been reported earlier in coupled neurons due to multiple time-scales [38] [39]. But we propose that in the present study the inhibitory coupling causes MMOs in HR neurons.
4. Another state that we observe is activity death. Now as the average degree in this case very high, the system is very prone to go into activity death even for $\beta \sim 0.15$. We therefore observe several activity death states (AD-1, AD-2, AD-3, AD-4, AD) in these networks. The sparse excitatory coupling in the module prevents this from happening provided the α is very high.

The spatio-temporal dynamics of this network in shown in figures 4.7 and 4.8, the $\alpha - \beta$ parameter plane is depicted in figure 4.9.

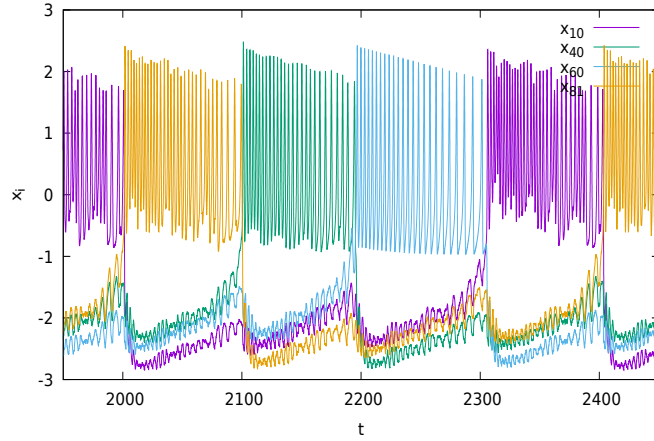


Figure 4.7: Mixed-mode oscillations observed in DIN. The figure has been plotted for $\alpha = 0.3$ and $\beta = 0.1$ and consists of the time series of 4 neurons belonging to different modules. We find that each individual neuron exhibits small and large amplitude bursts.

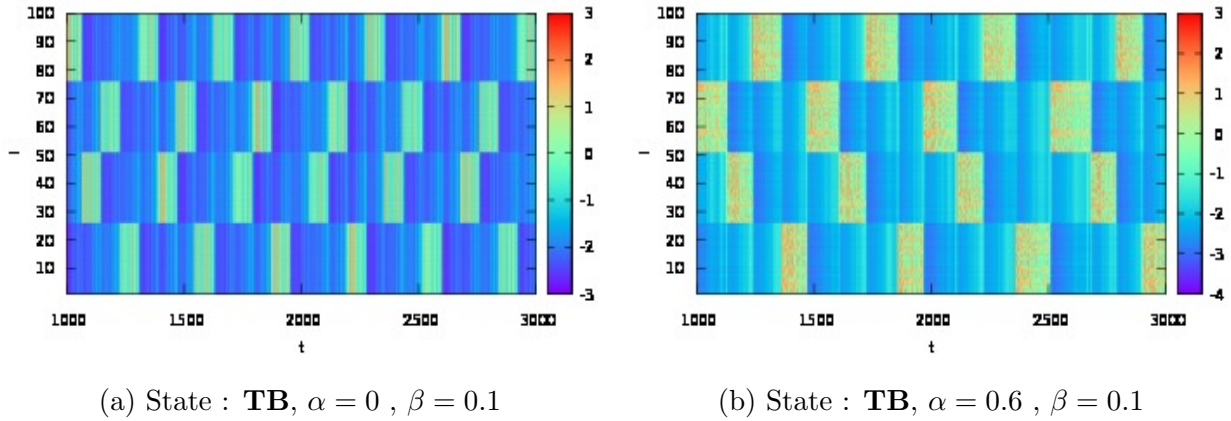


Figure 4.8: Travelling bursts in the modular network. (a) For $\alpha = 0$ the spikes inside each burst are completely synchronized. (b) For $\alpha > 0$ the spikes inside the burst become irregular. Bursting of neurons in each module is phase synchronized, but each module bursts successively after the other appearing dynamically as travelling bursts.

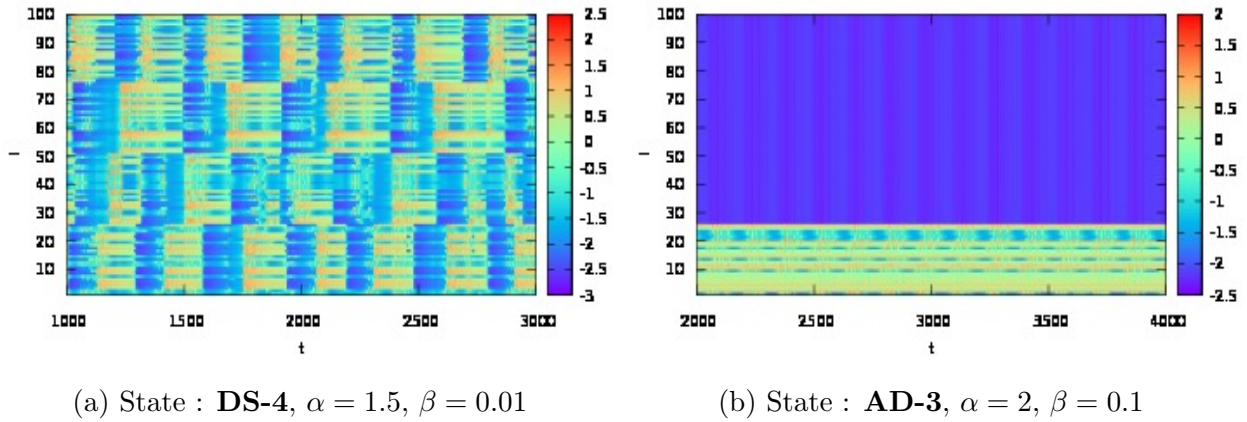


Figure 4.9: (a) Desynchronized State, (b) Activity Death State. High value of α desynchronizes the network.

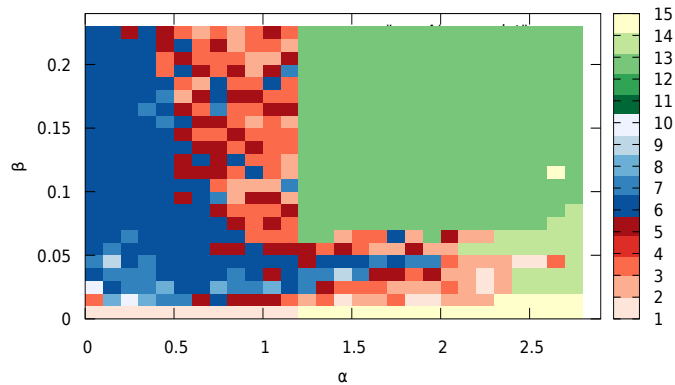


Figure 4.10: $\alpha - \beta$ parameter plane for Ω_2 . Red shades correspond to Desynchronised States, Blue shades corresponds to Phase Synchronized States, Green shades corresponds to Activity death states. The numbers given in the vertical band represent the dynamical states: 1-DS-4, 2-DS-3, 3-DS-2, 4-DS-2,P-2, 5-DS-1, 6-TB, 7-PS-2, 8-PS-2,2, 9-PS-3, 10-PS-4, 11-AD-1, 12-AD-2, 13-AD-3, 14-AD-4, 15-AD

Chapter 5

Conclusions

In the study presented in this thesis, we essentially consider three different models of networks consisting of Hindmarsh-Rose Neurons with the model: mutually coupled neurons with differing time-scales, ring of coupled neurons with spatially varying time-scales, and modular network consisting of excitatory and inhibitory synapses.

We summarize our main results in each of these models below :

- **Mutually Coupled Slow and Fast Neurons:**

1. Unlike the general system of nonlinear oscillators mentioned in [13], mutually coupled slow and fast neurons do not go into a state of amplitude death. We observe that the system goes into an amplitude death only because of a nonlinear synaptic coupling function for very high coupling strength. This is in accordance with reported results on amplitude death for nonlinear coupling [40]. We however observe a very sharp transition to a new state marked by very low amplitude oscillation termed as *Activity Death State*.
2. Differing time-scales between the two neurons results in a *Frequency Synchronized State* where the emergent frequency is lower than the average value of the intrinsic frequencies of the coupled neurons. This phenomenon is termed as *Frequency Suppression*. Suppression of the frequencies happens irrespective of the intrinsic dynamics of the individual systems. This phenomenon has relevance in the case of neurons as neuronal systems encode information based on the frequency of firing

or bursting of the individual neurons.

- **Ring of Neurons with differing time-scales:**

1. In the case of a linear chain of neurons with periodic boundary conditions, with the neurons having a linearly decreasing time-scale in space, we find for low values of coupling frequency synchronized clusters occur in the whole network. Now these clusters are dependent on the difference in time-scale η between two adjacent systems and also on the number of systems present. The synchronized clusters are lost when the difference in time-scales of adjacent systems is very small.
2. As the nonlinear coupling strength increases the discrete synchronized clusters in the whole ring collapse into a single *Synchronized Frequency Suppressed State*. This happens at a constant value of g_s for all values of N and $\Delta\eta$. So essentially the whole network is bursting at a single frequency even if all the individual neurons are in different time-scales. This frequency is very less compared to the intrinsic frequencies.

- **Modular networks with excitatory and inhibitory coupling**

1. We consider two different networks in this particular case - *Associative Excitatory Network (AEN)* and *Disassociative inhibitory Network (DIN)*. In both the cases we study the dynamics of the chaotic bursting HR neurons with excitatory intra-modular coupling α and inhibitory inter-modular coupling β . We classify the dynamics of the system into 3 major states - *Desynchronized, Phase Synchronized and Activity Death*. Each state can be classified into 5 sub-states based on the relative dynamics of each module. We plot the spatio-temporal dynamics and the parameter plane $\alpha - \beta$ to quantify the possible dynamical states in both cases.
2. In the case of AEN, since the whole network has randomly placed synapses, we find that the general dynamics of the system is a desynchronized state. This essentially means that the neurons present in each module are desynchronized in phase. However carefully tuning the coupling parameters we can obtain phase synchronized states, where some modules are in same phase and the others are in off phase, or desynchronized. This type of modular phase synchronization is an interesting emergent phenomenon in neuronal networks.
3. In case of DIN, we observe an interesting emergent phenomenon called *traveling bursts*. The neurons in each module tend to synchronize in phase and they

burst successively one after the other. In real-time the bursts appear as if they are travelling throughout the network. Moreover these inhibitory neurons show mixed-mode oscillations consisting of low and high amplitude bursts. We propose this type of behaviour is emergent from the inhibitory coupling between the systems unlike the presence of multiple timescales in individual system reported earlier [38].

4. In both types of modular networks, the common phenomenon observed is activity death, that occurs if the coupling strength (excitatory α or inhibitory β) is high enough. Interestingly if the system reaches AD due to inhibitory/ excitatory coupling, the other type of coupling can revive the system back to a de-synchronized state. In this way, the threshold required by the system is higher in the presence of hybrid coupling considered here.

5.1 Future Prospects

Our work with HR neurons in modular networks have given us several insights into the various dynamical states possible in neuronal networks. We have classified the dynamics of the network into 15 different states comprising of desynchronized, synchronized and activity death states. However there are several aspects of this model which can be explored further.

- In this study we consider networks of size $N = 100$. Now studying the dynamics of such a high dimensional system gives us a good look at the qualitative picture of the dynamics as we can easily average over the ensembles without losing a lot of information on the details of the individual dynamics of the neurons. But working on such a high dimensional system is computationally intensive. Also most modular networks of neurons found in the natural systems usually consists of 15-20 neurons in a cluster making the network sizes upto 60. So we can reduce this system to networks with less neurons and more efficiently explore the dynamics of the network.
- We classify the dynamical states in our model based on the number of phase synchronized, desynchronized or AD modules in the network. We take the number of modules to be $M = 4$ giving us 15 possible state. So changing the number of modules, we can use this scheme to deduce the dynamics of actual neuronal networks in the brain.

We can even look at aspects of coding information for various inputs in these modular networks.

- We can explore the effect of having multiple time-scales in the modules. We have done some preliminary studies on this by assigning a value of η_m to each module in the case of assortative excitatory networks, taking:

$$\boldsymbol{\eta} = [1, \eta, 1, 1] \tag{5.1.1}$$

Thus for $\eta = 0.5$, one of the modules is slower than the other three. So the system essentially has a forced asymmetry which can lead to interesting spatio-temporal patterns and dynamical behaviour. With time-scale mismatch we can generate patterns of different frequency synchronized state emerging in the network of randomly coupled neurons.

The present study with further extensions will certainly enhance our understanding of the basic dynamics underlying the complexity of the brain and point towards ways of unravelling its mysteries.

Bibliography

- [1] EM Izhikevich. *Dynamical systems in neuroscience*. 2004.
- [2] A. L. Hodgkin and A. F. Huxley. A quantitative description of membrane current and its application to conduction and excitation in nerve. *Bulletin of Mathematical Biology*, 52(1-2):25–71, 1990.
- [3] Erik Fransén, Angela A. Alonso, Clayton T. Dickson, Jacopo Magistretti, and Michael E. Hasselmo. Ionic mechanisms in the generation of subthreshold oscillations and action potential clustering in entorhinal layer II stellate neurons. *Hippocampus*, 14(3):368–384, 2004.
- [4] Richard FitzHugh. Impulses and Physiological States in Theoretical Models of Nerve Membrane. *Biophysical Journal*, 1(6):445–466, 1961.
- [5] J. Nagumo, S. Arimoto, and S. Yoshizawa. An Active Pulse Transmission Line Simulating Nerve Axon*. *Proceedings of the IRE*, 50(10):2061–2070, 1962.
- [6] K. Rajagopal. A model for the nerve impulse propagation using two first-order differential equations, 1983.
- [7] J. L. Hindmarsh and R. M. Rose. A model of neuronal bursting using three coupled first order differential equations, 1984.
- [8] Giacomo Innocenti, Alice Morelli, Roberto Genesio, and Alessandro Torcini. Dynamical phases of the Hindmarsh-Rose neuronal model: Studies of the transition from bursting to spiking chaos. *Chaos*, 17(4), 2007.
- [9] Roberto Barrio, M. Angeles Martínez, Sergio Serrano, and Andrey Shilnikov. Macro- and micro-chaotic structures in the Hindmarsh-Rose model of bursting neurons. *Chaos (Woodbury, N.Y.)*, 24(2):023128, 2014.
- [10] Marco Storace, Daniele Linaro, and Enno De Lange. The Hindmarsh-Rose neuron model: Bifurcation analysis and piecewise-linear approximations. *Chaos*, 18(3), 2008.
- [11] Jonq Juang and Yu Hao Liang. Cluster synchronization in networks of neurons with chemical synapses. *Chaos*, 24(1), 2014.

- [12] Nikolai F. Rulkov. Modeling of spiking-bursting neural behavior using two-dimensional map. *Physical Review E - Statistical, Nonlinear, and Soft Matter Physics*, 65(4), 2002.
- [13] Kajari Gupta and G Ambika. Amplitude death in coupled slow and fast dynamical systems. 2014.
- [14] Z M Ge and C C Chen. Phase synchronization of coupled chaotic multiple time scales systems. *Chaos, Solitons & Fractals*, 20(3):639–647, 2004.
- [15] T. Pereira, M. S. Baptista, and J. Kurths. General framework for phase synchronization through localized sets. *Physical Review E - Statistical, Nonlinear, and Soft Matter Physics*, 75(2):1–12, 2007.
- [16] Ines Grozdanović, Kristina Todorović, Nebojša Vasović, Nikola Burić, and Nataša Trišović. Interplay between internal delays and coherent oscillations in delayed coupled noisy excitable systems. *International Journal of Non-Linear Mechanics*, 73:121–127, 2015.
- [17] Carlo Nicolini and Angelo Bifone. Modular structure of brain functional networks: breaking the resolution limit by Surprise. *Scientific Reports*, 6(January):19250, 2016.
- [18] M. S. Santos, J. D. Szezech, F. S. Borges, K. C. Iarosz, I. L. Caldas, A. M. Batista, R. L. Viana, and J. Kurths. Chimera in a neuronal network model of the cat brain. pages 1–5, 2016.
- [19] Johanne Hizanidis, Nikos E. Kouvaris, Zamora-López Gorka, Albert Díaz-Guilera, and Chris G. Antonopoulos. Chimera-like States in Modular Neural Networks. *Scientific Reports*, 6(January):19845, 2016.
- [20] Peter Ashwin, Stephen Coombes, and Rachel Nicks. Mathematical Frameworks for Oscillatory Network Dynamics in Neuroscience. *The Journal of Mathematical Neuroscience*, 6(1):2, 2016.
- [21] C. A S Batista, E. L. Lameu, A. M. Batista, S. R. Lopes, T. Pereira, G. Zamora-Lopez, J. Kurths, and R. L. Viana. Phase synchronization of bursting neurons in clustered small-world networks. *Physical Review E - Statistical, Nonlinear, and Soft Matter Physics*, 86(1):1–12, 2012.
- [22] Igor Belykh, Enno De Lange, and Martin Hasler. Synchronization of bursting neurons: What matters in the network topology. *Physical Review Letters*, 94(18):1–4, 2005.
- [23] Bidesh K. Bera, Dibakar Ghosh, and M. Lakshmanan. Chimera states in bursting neurons. *Physical Review E - Statistical, Nonlinear, and Soft Matter Physics*, 93(1):1–9, 2016.
- [24] Soumen Majhi, Matjaz Perc, and Dibakar Ghosh. Chimera states in uncoupled neurons induced by a multilayer structure. *Nature Publishing Group*, (September):1–11, 2016.

- [25] CJ Cornelis J Stam and Jaap C JC Reijneveld. Graph theoretical analysis of complex networks in the brain. *Nonlinear biomedical physics*, 1:3, 2007.
- [26] Gorka Zamora-López, Eleonora Russo, Pablo M Gleiser, Changsong Zhou, and Jürgen Kurths. Characterizing the complexity of brain and mind networks. *Philosophical transactions. Series A, Mathematical, physical, and engineering sciences*, 369:3730–3747, 2011.
- [27] Rodrigo Echeveste and Claudius Gros. Drifting States and Synchronization Induced Chaos in Autonomous Networks of Excitable Neurons. *Frontiers in Computational Neuroscience*, 10(September):1–11, 2016.
- [28] Tilman Kispersky, John A. White, and Horacio G. Rotstein. The mechanism of abrupt transition between theta and hyper-excitable spiking activity in medial entorhinal cortex layer II stellate cells. *PLoS ONE*, 5(11), 2010.
- [29] Zaneta Navratilova, Lisa M. Giocomo, Jean Marc Fellous, Michael E. Hasselmo, and Bruce L. McNaughton. Phase precession and variable spatial scaling in a periodic attractor map model of medial entorhinal grid cells with realistic after-spike dynamics. *Hippocampus*, 22(4):772–789, 2012.
- [30] Sang Yoon Kim and Woochang Lim. Noise-induced burst and spike synchronizations in an inhibitory small-world network of subthreshold bursting neurons. *Cognitive Neurodynamics*, 9(2):179–200, 2015.
- [31] Pablo M. Gleiser and Victor I. Spoomaker. Modelling hierarchical structure in functional brain networks. *Philosophical Transactions of the Royal Society A: Mathematical, Physical and Engineering Sciences*, 368(1933):5633–5644, 2010.
- [32] Collins Assisi, Mark Stopfer, and Maxim Bazhenov. Using the structure of inhibitory networks to unravel mechanisms of spatiotemporal patterning. *Neuron*, 69(2):373–386, 2011.
- [33] David Meunier, Renaud Lambiotte, and Edward T. Bullmore. Modular and hierarchically modular organization of brain networks. *Frontiers in Neuroscience*, 4(DEC):1–11, 2010.
- [34] Richard H Rand, Avis H Cohen, and Philip J Homles. System of coupled oscillators as a model of central pattern generators, 1988.
- [35] J R Gibson, M Beierlein, and B W Connors. Two networks of electrically coupled inhibitory neurons in neocortex. *Nature*, 402(6757):75–79, 1999.
- [36] Aaron Clauset. The stochastic block model. *Lecture Notes*, (November):1–6, 2013.

- [37] Ewanson L. Lameu, Fernando S. Borges, Rafael R. Borges, Kelly C. Iarosz, Iberê L. Caldas, Antonio M. Batista, Ricardo L. Viana, and Jürgen Kurths. Suppression of phase synchronisation in network based on cat's brain. *Chaos*, 26(4), 2016.
- [38] Jonathan Rubin and Martin Wechselberger. The selection of mixed-mode oscillations in a Hodgkin-Huxley model with multiple timescales. *Chaos*, 18(1):1–12, 2008.
- [39] Roman Nagornov, Grigory Osipov, Maxim Komarov, Arkady Pikovsky, and Andrey Shilnikov. Mixed-mode synchronization between two inhibitory neurons with post-inhibitory rebound. *Communications in Nonlinear Science and Numerical Simulation*, 36:175–191, 2016.
- [40] Awadhesh Prasad, Mukeshwar Dhamala, Bhim Mani Adhikari, and Ramakrishna Ramaswamy. Amplitude death in nonlinear oscillators with nonlinear coupling. *Physical Review E - Statistical, Nonlinear, and Soft Matter Physics*, 81(2):2–5, 2010.